

Reversible supramolecular modification of surfaces

THÈSE N° 6861 (2015)

PRÉSENTÉE LE 27 NOVEMBRE 2015

À LA FACULTÉ DES SCIENCES ET TECHNIQUES DE L'INGÉNIEUR
LABORATOIRE DES DISPOSITIFS NANOÉLECTRONIQUES
PROGRAMME DOCTORAL EN MICROSYSTÈMES ET MICROÉLECTRONIQUE

ÉCOLE POLYTECHNIQUE FÉDÉRALE DE LAUSANNE

POUR L'OBTENTION DU GRADE DE DOCTEUR ÈS SCIENCES

PAR

Negar MORIDI

acceptée sur proposition du jury:

Prof. S. Lacour, présidente du jury
Prof. M. A. Ionescu, Prof. P. Shahgaldian, directeurs de thèse
Prof. Ph. F.-X. Corvini, rapporteur
Prof. T. Bruno, rapporteur
Prof. S. Gerber, rapporteuse



ÉCOLE POLYTECHNIQUE
FÉDÉRALE DE LAUSANNE

Suisse
2015



**Reversible supramolecular
modification of surfaces**

Negar Moridi

می کوش به هر ورق که خوانی... تا معنی آن تمام دانی
- نظامی گنجوی

*To my parents
Mehri & Hossein*

Acknowledgements

I would like to express my sincere gratitude to Prof. Dr. Shahgaldian, for the patient guidance, encouragement and motivation he has provided me throughout my studies. He has been supportive since the first day I began working as an undergraduate student in his research group and he has always been available for discussions and advices. He taught me a lot about scientific research.

I would like to express my appreciation to my advisor at Ecole Polytechnique Fédérale de Lausanne, Prof. Dr. Mihai Adrian Ionescu. I am thankful for the freedom he granted to me during my research work.

I would like to thank Prof. Dr. Stéphanie Lacour, Prof. Dr. Sandrine Gerber, Prof. Dr. Philippe F.-X. Corvini and Prof. Dr. Therrien Bruno for accepting to be member of my thesis committee.

I would like to acknowledge Prof. Dr. Uwe Pieles and his research team, especially Markus, Lucy and Théo, for their continuous support and help. I am also thankful to Dr. Martin Oeggerli to colour the cover figure of my manuscript. I would like to thank Peter Spies from bio-analytics department, for helping me with surface plasmon resonance binding assays.

This research work could not have been completed without the great support that I have received from my friends and colleagues with whom I have shared moments of tension but also of enthusiasm. Special thanks go to Alessandro, Mohamed, Rita, Ludovico, Sabine and Mina.

I would like to express my deepest gratitude to my family. This research work would not have been possible without their love, endless support, and sacrifices. I would like to dedicate this thesis to my parents, Mehri and Hossein, whose love and guidance are with me in all my pursuits. I would like to thank my sister, brother, my lovely nieces, Neda, Mohssen, Nathalie and Maya, for their faithful supports throughout my life. I would also like to thank

my dear husband, Christian, for his endless patience and encouragement during these years. This last word of acknowledgment I have saved for my beloved grandfather, Jalal Jamali, who had a very important role in my life.

Abstract

Enzymes are biocatalysts widely used in a large number of industrial biotechnology processes as they offer clear advantages over their chemical counterparts. Indeed, enzymes often show high substrate selectivity along with elevated turnover rates. Enzymatic catalysis usually functions under mild conditions of temperature, pressure and acidity. However, the industrial application of enzymes is often limited by their limited stability under operational conditions. Moreover, due to high water solubility of enzymes it is challenging to confine them in a flow reactor system.

In order to circumvent these limitations, we have developed a supramolecular strategy that allows the reversible immobilization of active enzyme-polymer conjugates at the surface of filtration membranes. It is based on multivalent host-guest inclusion interactions between the membrane surface and a soluble enzyme-polymer conjugate. Cyclodextrins (CDs) as "host" molecules are covalently attached at the surface of polyethersulfone membranes and a multivalent water-soluble polymer is synthesized as a "guest" molecule. We demonstrate that while this supramolecular surface modification is stable under operational conditions and allows for efficient bio-catalysis, it can be straightforwardly reverse by competitive host-guest interactions.

The first part of this manuscript is dedicated to a literature review on selected topics. As the supramolecular strategy we have developed in the course of this PhD research work is based on the use of cyclodextrins as supramolecular host molecules, the first part of this literature review focuses on the physico-chemical characteristics of this class of macrocycles. A special emphasis is done on their ability to form host-guest multivalent inclusion complexes. In this context, we describe the concept of multivalency and the underpinning essential thermodynamic principles, which can be apply to design controllable, directional, and selective self-assemblies.

In the second part of this manuscript, we present our strategy to bio-functionalize polymeric membrane surfaces using multivalent reversible inclusion reactions. In more details, the chemical strategy to introduce CD macrocycles, in a covalent fashion, at the surface of the polymeric material is discussed. The synthesis and characterization of an enzyme-polymer conjugate, possessing multiple chemical functional groups (*i.e.* adamantyl) able to form inclusion complexes with CDs, is presented. It is demonstrated that this supramolecular strategy could be applied to the reversible immobilization of an active enzyme at the surface of polyethersulfone membranes.

A similar strategy is applied to the reversible bio-functionalization of gold surfaces and used to prepare sensor chips for surface plasmon resonance (SPR) experiments. Self-assembled monolayers of CDs derivatives are prepared on the surface of a gold sensor chip. A water-soluble protein-polymer conjugate, possessing multiple adamantyl moieties, is synthesized. The supramolecular reversible binding of this new conjugate on the chemically modified SPR chip is demonstrated. The possibility to use this system for antigen/antibody biosensing experiment is successfully confirmed.

Keywords: Polymer, Self-assembly, Supramolecular chemistry, Surface chemistry, Enzyme catalysis

Résumé

Les enzymes sont des catalyseurs biologiques qui sont utilisées dans de nombreux procédés industriels car elles offrent un avantage certain sur leurs équivalents chimiques. En effet, les enzymes possèdent généralement une sélectivité élevée pour leur substrat qu'elles transforment avec de haut taux de conversion. Les réactions catalysées par des enzymes se déroulent habituellement dans des conditions mesurées en termes de température, pression et acidité. Cependant, les applications industrielles impliquant des enzymes sont souvent limitées par la stabilité de ces biomolécules en conditions opérationnelles. De plus, du fait de la solubilité élevée des enzymes en milieu aqueux, le confinement à l'intérieur d'un réacteur en flux continu représente un défi.

Afin de dépasser ces limites, nous avons développé une stratégie supramoléculaire basée sur des interactions hôte-invité qui permet l'immobilisation d'un conjugué polymère-enzyme, soluble dans l'eau, à la surface de membranes de filtration. Cette stratégie se base sur l'utilisation de cyclodextrines (CDs), agissant en tant que molécules « hôtes », liées de façon covalente à la surface de la membrane du polyéthersulfone. Un polymère multivalent et soluble dans l'eau est synthétisé pour jouer le rôle de molécule « invité ». Nous démontrons comment la modification supramoléculaire de la surface, stable dans les conditions opérationnelles, permet une biocatalyse efficace et peut être aisément relarguée par l'intermédiaire d'interactions hôtes-invités compétitives.

La première partie du manuscrit est dédiée à une étude bibliographique menée sur les sujets suivants. La stratégie supramoléculaire développée durant ce travail de recherche de doctorat étant basée sur l'utilisation de la cyclodextrine en tant que molécule hôte, la première partie de la bibliographie se concentre sur les caractéristiques physico-chimiques de cette famille de macrocycles. L'accent est mis sur leur habilité à former des complexes d'inclusion multivalents hôte-invité. Dans ce contexte, nous décrivons le concept de multivalence et ces fondements essentiels en terme de thermodynamique, qui peuvent être appliqués pour élaborer de façon contrôlée et sélective des entités auto-assemblées.

Dans la seconde partie du manuscrit, nous présentons notre stratégie pour bio-fonctionnaliser les surfaces de membranes de polymère en utilisant des réactions d'inclusion réversibles. La stratégie de synthèse pour introduire des macrocycles de cyclodextrine, de façon covalente, à la surface de ce polymère est aussi discutée en détail. La synthèse et la caractérisation du conjugué polymère-enzyme possédant plusieurs groupes fonctionnels (*i.e.* adamantane) capable de former des complexes d'inclusion avec la CD sont présentées. Il est établi que cette stratégie supramoléculaire peut être appliquée à l'immobilisation réversible d'enzymes actives à la surface de la membrane en polyéthersulfone.

Une stratégie similaire est appliquée pour la bio-fonctionnalisation réversible des surfaces d'or et utilisée pour préparer des capteurs pour des expériences de résonance de plasmon de surface. Les monocouches auto-assemblées de dérivés de CD ont été préparées à la surface d'un capteur d'or. Un conjugué protéine-polymère soluble dans l'eau et possédant des groupements adamantyls a été synthétisé. Le lien supramoléculaire et réversible de ce nouveau conjugué sur le biocapteur a été démontré. La possibilité d'utiliser ce système pour des expériences impliquant des biocapteurs antigène/anticorps a été confirmée avec succès.

Mots-clés: Polymère, Auto-assemblage, Chimie supramoléculaire, Chimie des surfaces, Catalyse enzymatique

Contents

Acknowledgements	vii
Abstract	ix
Résumé.....	xi
List of Figures.....	xv
List of Equations	xviii
Abbreviations	xix
Symbols	xxi
Chapter 1. State of the art	1
1.1. Cyclodextrins.....	2
1.1.1. Historical overview.....	2
1.1.2. Structural and physico-chemical characteristics of cyclodextrins.....	2
1.1.3. Industrial production of cyclodextrins	4
1.1.4. Formation of host-guest inclusion compounds.....	6
1.2. Multivalency	7
1.2.1. Thermodynamic principles of multivalent interactions	8
1.2.2. Multivalency in solution.....	12
1.2.3. Multivalency at interfaces.....	17
Chapter 2. Results and discussion.....	27
2.1. Reversible supramolecular modification of membrane surfaces	27
2.1.1. Covalent modification of PES membranes.....	28
2.1.2. Synthesis of the multivalent enzyme-polymer conjugate (MEP)	33
2.1.3. Surface attachment of the multivalent enzyme-polymer conjugates.....	37
2.2. Reversible supramolecular modification of surface resonance sensor (SPR) chip	44
2.2.1. Chemical modification of gold sensor chips.....	45
2.2.2. Synthesis of the multivalent BSA-polymer conjugate (MPP)	47
2.2.3. Assessment of the supramolecular binding of MPP on the chemically-modified SPR chips.....	48
Chapter 3. Experimental methods	53
3.1. General	53
3.2. Synthesis of the enzyme-polymer conjugate (MEP).....	53
3.3. Synthesis of the multivalent BSA-polymer conjugate (MPP).....	55
3.4. Synthesis of the <i>per</i> -6-iodo- β -cyclodextrin	55
3.5. Synthesis of the <i>per</i> -6-azido- β -cyclodextrin	55

3.6.	Synthesis of the <i>per</i> -6-amino- β -cyclodextrin	56
3.7.	Synthesis of 12-(thiododecyl)undecanoic acid	56
3.8.	Synthesis of heptakis{6-deoxy-6-[12(thiododecyl)undecanamido]}- β -CD	57
3.9.	Chemical modification of polyethersulfone filtration membranes	57
3.10.	Chemical modification of gold sensor chip (NH-CD-Au)	57
3.11.	Glucose oxidase method	58
3.12.	<i>Ortho</i> -nitrophenyl- β -galactoside (ONPG) enzymatic assay	58
3.13.	Microscopic characterization	58
3.14.	Spectroscopic ellipsometry measurements.....	59
Chapter 4.	Conclusion	61
References.....		65
Curriculum Vitae.....		71

List of Figures

Figure 1.1: Chemical structures of α , β and γ -CDs	3
Figure 1.2: X-ray crystal structure of α -, β - and α -CD, water molecules are omitted for clarity.....	3
Figure 1.3: Diagram of solvent processes for industrial production of CDs.....	5
Figure 1.4: Diagram of non-solvent processes for industrial production of β -CDs	6
Figure 1.5: inclusion complex of a hydrophobic guest molecule and a CD in water.....	6
Figure 1.6: Schematic representation of a) monovalent interactions, b) multiple monovalent interactions and c) multivalent interactions.....	8
Figure 1.7: Schematic representation of different topologies of multivalent interactions	10
Figure 1.8: examples of multivalent systems using zinc-porphyrin-pyridyl system; a) the pre-organized host; b) using a linear bis(Zn porphyrin) which is less pre-organized	12
Figure 1.9: The trivalent equilibrium interaction between tris(crown ether) and the tris-ammonium ion.....	13
Figure 1.10: A schematic representation of the equilibration supramolecular interaction between the tris-crown ether and the tris-ammonium ion, involving entities that are triply-, doubly-, and singly-bound, as well as free.....	14
Figure 1.11: Multivalent host (trivalent vancomycin) and guest (D Ala D Ala trimer) entities.....	15
Figure 1.12: Multivalent interaction of a β -CD dimer as a host and a bis(adamantyl) guest.....	16
Figure 1.13: Left, multivalent host (β -CD dimers tethered) and guest (toluidino-2-naphthalene sulfonate) entities; right, the plot of binding affinity versus inverse cubic tether length for complexation of the toluidino-2-naphthalene sulfonate and CD dimer with variable tether length ..	16
Figure 1.14: A schematic representation of the photo-switchable supramolecular interaction between a β -CD dimers and multivalent porphyrin guest.....	17
Figure 1.15: chemical structure of some selective β -CD SAMs building blocks	18
Figure 1.16: Formation of an organized monolayer of an amino derivative of β -CD (5) on a silicon oxide surface. i) sodium bis(2-methoxyethoxy)aluminumhydride; ii) 1,4-phenylene diisothiocyanate; iii) NH-CD	19
Figure 1.17: Atomic force microscopy images of the μ CP Fc-functionalized dendrimers patterns at β -CD SAMs on glass substrates a) before rinsing; b) after rinsing with water; c) schematic representation of induced electrochemical desorption of guest molecules from molecular printboards using scanning electrochemical microscopy	20
Figure 1.18: Schematic representation of a) conjugation of cysteine-functionalized Fcs and thioester-functionalized yellow fluorescent proteins; followed by covalent locking of two Fc-YFPs; b) immobilization of divalent Fc-YFPs onto thioether-functionalized β -CD monolayers	21
Figure 1.19: Schematic representation of the chemical structures of the building blocks and scheme for the step-wise assembly process.....	22

Figure 1.20: a) Chemical structure of coumarin, <i>per</i> -azido- β -CDs, labelled diadamantyl guest and azide-functionalized dye; b) schematic representation of the patterned alkyne- β -CD monolayer prepared by μ CP of <i>per</i> -azido- β -CDs onto coumarin terminated monolayers	23
Figure 1.21: SEM micrographs of nano-imprint lithography-patterned CD-layers followed by supramolecular host-guest assemblies of a) fifteen bilayers of adamantyl-functionalized dendrimers and CD functionalized Au NPs with 200 nm dot features; b) two bilayers (with 150 nm wide grids); c) one bilayer of the adamantyl functionalized dendrimers and CD functionalized SiO ₂ NPs with 60 nm dots pattern forms; d) single NPs (60 nm) on a periodic pattern	24
Figure 1.22: Specific molecular recognition visualized at macroscopic scale	25
Figure 2.1: Chemical structure of polyethersulfone (PES)	28
Figure 2.2: (a) Schematic representation of the synthetic route to introduce carboxylic functions at the surface of PES membranes in a micro-patterned fashion; FTIR absorbance spectra characterization of (b) bare PES membrane and (c) PES membranes modified with acrylic acid.	29
Figure 2.3: Assessment of carboxylic acid immobilization at the surface of the AA-PES membranes; (a) measurements of relative intensities of carbonyl bands of AA-PES membranes as a function of UV irradiation time; (b) measurements of water flow through AA-PES membranes as a function of UV irradiation time.....	30
Figure 2.4: FE-SEM micrographs of (a) PES and (c) AA-PES. AFM tapping mode micrographs (25 μ m scan range) of (b) PES and (d) AA-PES. Scale bars represent 5 μ m.....	31
Figure 2.5: Synthetic route to NH-CD	32
Figure 2.6: EDC reacts with carboxylic acids to create an <i>O</i> -acylisourea intermediate. In the presence of NH-CD, an amide bond is formed with release of an isourea by-product.	32
Figure 2.7: (a) Schematic representation of the synthetic route to introduce NH-CDs at the surface of AA-PES membranes in a micro-patterned fashion; (b) FTIR absorbance spectra of NH-CD-PES membrane; (c) FE-SEM micrographs of PES; (d) AFM tapping mode micrograph (25 μ m scan range) of a NH-CD-PES. Scale bars represent 5 μ m.....	33
Figure 2.8: Synthetic route to adamantyl acrylamide.....	34
Figure 2.9: Synthetic route to a soluble guest polymer	34
Figure 2.10: (a) Synthetic route to the fluorescently labelled MEP; (b) Schematic representation of the multivalent supramolecular binding of MEP to covalently immobilized CDs on the membrane surface.	36
Figure 2.11: Synthetic route to fluorescently labelled MEP _{ref}	37
Figure 2.12: Fluorescence micrographs of the NH-CD-PES membrane, (a) before (NH-CD-PES) and (b) after incubation in MEP solution; (c) after incubation in a solution of β -CD and (d) after a second incubation in MEP solution. Scale bars represent 200 μ m.	38
Figure 2.13: Measurements of ONPG conversion rates at the surface of membranes in a batch process after incubation of NH-CD-PES membranes in MEP solution, followed by incubation in a β -CD solution as a competitor host. The procedure was repeated five times.	39
Figure 2.14: Schematic representation of the setup used for continuous filtration process	40
Figure 2.15: Measurements of ONPG conversion rates at the surface of the MEP-modified membranes in batch (●) and continuous (○) processes using increasing concentrations of ONPG.	41
Figure 2.16: Measurements of lactose conversion rates at the surface of membranes after filtration of milk serum solution through the MEP-modified membranes, followed by filtration of a β -CD solution as a competitor host. The procedure was repeated five times.	42
Figure 2.17: Schematic representation of a multivalent supramolecular binding of an antigen-polymer conjugate to covalently immobilized CDs on a SPR sensor chip surface.	45

Figure 2.18: (a) Synthetic route to 12-(thiododecyl)undecanoic acid; (b) synthetic route to heptakis(6-deoxy-6-[12(thiododecyl)undecanamido]- β -CD; <i>O</i> -Benzotriazol-1-yl- <i>N,N,N',N'</i> -tetramethyluronium tetrafluoroborate (TBTU) was used as an activating agent	46
Figure 2.19: Schematic representation of a SAM of dialkylsulfide derivative of β -CD on a gold surface	47
Figure 2.20: Synthetic route to MPP.....	48
Figure 2.21: Binding sensogram of MPP, values are expressed in arbitrary units and normalized to zero at the beginning of the injection.....	48
Figure 2.22: Binding sensogram of specific AntiBSA-MPP interactions	49
Figure 2.23: AntiBSA dissociation sensogram after loading of glycine solution	50
Figure 2.24: AntiBSA dissociation sensogram after injection of β -CD solution.....	50
Figure 2.25: Binding sensogram of the regenerated Au sensor chip	51

List of Equations

Equation 1.1: Association constant of a host-guest complex	7
Equation 1.2: Probabilities for j receptor sites to bind an n -valent receptor	8
Equation 1.3: Degree of cooperativity	9
Equation 1.4: Magnitude of multivalent associations relative to monovalent bindings	9
Equation 1.5: Enhancement factor	9
Equation 1.6: Avidity enhancement of a multivalent binding	10
Equation 1.7: Association constant for the n -valent interaction	11
Equation 1.8: Effective molarity	11

Abbreviations

AA	Acrylic acid
AA-PES	AA-modified PES
AFM	Atomic force microscopy
AIBN	Azobisisobutyronitrile
AlkPh	Alkaline phosphatase
AntiBSA	Bovine serum albumin antibody
ATR	Attenuated total reflection
AU	Arbitrary units
BSA	Bovine serum albumin
bt-AlkPh	Biotinylated alkaline phosphatase
CD-Au	NH-CD-modified Au substrate
CDs	Cyclodextrins
CGTase	Cyclodextrin glucosyltransferase
^D Ala ^D Ala	D-alanine-D-alanine
EDC	1-Ethyl-3-(3-dimethylaminopropyl)carbodiimide
EM	Effective molarity
Fc	Ferrocene
Fc-YFPs	Ferrocene-tagged yellow fluorescent proteins
FE-SEM	Field-emission scanning electron microscopy
FITC	Fluorescein isothiocyanate
FTIR	Fourier-transform infrared spectroscopy
G	Guest
GPC	Gel-permeation chromatography

MALDI-TOF	Matrix-assisted laser desorption/ionization time of flight mass spectroscopy
MEP	Water-soluble enzyme-polymer conjugate
MPP	Multivalent antigen-polymer conjugate
MPP-Au	MPP-modified Au substrate
MEP _{ref}	Water soluble reference polymer
MWCO	Molecular weight cut-off
NH-CD	Heptakis(6-deoxy-6-amino)- β -cyclodextrin
NH-CD-PES	NH-CD-modified PES
ONPG	<i>Ortho</i> -nitrophenyl- β -galactoside
PCSA	Polarizer-compensator-sample-analyser
PES	Polyethersulfone
RAFT	Reversible addition-fragmentation transfer
rhodamine Ad ₂	Sulforhodamine B acid chloride-labelled divalent adamantyl guest
RI	Refractive index
RMS	Root mean square roughness
SAMs	Self-assembled monolayers
SAv	Biotin-Streptavidin
S _N 2	Nucleophilic substitution
SPR	Surface plasmon resonance
sulfo-NHS	N-hydroxysulfosuccinimide
TBTU	<i>O</i> -Benzotriazol-1-yl- <i>N,N,N',N'</i> -tetramethyluronium tetrafluoroborate
μ CP	Micro-contact printing
β -CD	β -cyclodextrin
β -gal	β -galactosidase

Symbols

C_{eff}	Effective concentration
K_n	Association constant for the n -valent interaction
w_i	Weight coefficient
α	Cooperativity factor
β	Enhancement factor
ΔG°_{inter}	Free energy change for the first receptor-ligand interaction
ΔG°_{intra}	Free energy change for each additional interaction in the multivalent complex
ΔG_{mono}	Free binding enthalpy of a monovalent system
ΔG_{multi}	Free binding enthalpy of a multivalent system
$\Delta S_{complex}$	Entropy change for the host-guest complexation
σ	Symmetry number of a molecule
Ω_i	A combinatorial factor reflecting the probability of association and dissociation of individual ligands

Chapter 1. State of the art

Multivalent interactions are defined as non-covalent interactions between multivalent receptors and ligands. Multivalent interactions usually result in higher binding strength than the sum of the corresponding monovalent interactions. Multivalency is an important principle used by nature and chemists for achieving strong, yet reversible interactions.

In supramolecular chemistry, the concept of multivalency can be used to design controllable, directional, and selective self-assemblies.^{1,2} Cyclodextrins (CDs) are one of the classes of molecules widely used to design multivalent systems on surfaces. One of the important features of CDs is their ability to form complexes with variety of hydrophobic molecules.^{3,4} CDs do not possess an intrinsic ability to self-assemble at interfaces or to bind covalently to surfaces. Nevertheless, a series of rational chemical modifications of the CD macrocycle have proven successful in the production of CDs that can react covalently with surfaces.⁵⁻⁷ The concept of multivalency can be applied to modify solid surfaces in a stable and reversible fashion.⁸⁻¹¹

In the present research work, we developed a supramolecular strategy based on multivalency that can allow stable but yet reversible anchoring of biocatalysts at the surface of polymeric membranes. We applied the concept of multiple-point interactions using a polymeric multivalent guest (adamantyl bearing polymer) and a host molecule (β -cyclodextrin, β -CD) immobilized on the surface of a polymeric filtration membrane.

In the first part of this chapter, a general overview about the history of CDs and their industrial production is given. Furthermore, physico-chemical characteristics of CDs and their ability to form host-guest inclusion compounds are discussed. The second part of this chapter is devoted to an overview about the concept of multivalency and the underlying thermodynamic principles. Selected important research works on different multivalent systems using CDs in solution and at interfaces are described and discussed.

1.1. Cyclodextrins

1.1.1. Historical overview

The history of CDs starts in France at the end of 19th century with the research of Antoine Villiers on the action of enzymes on different carbohydrates. In 1891, reporting his results on the degradation of potato starch by *Bacillus amylobacter* to the French National Academy of Sciences, he demonstrated that after processing one kilogram of starch under the action of ferments, three grams of a carbohydrate with the chemical formula of “C₁₂H₁₀O₁₀+3HO” was crystallized in the form of elongated, shiny crystals.¹² He proposed the name “cellulosine” due to the similarities of this substance with cellulose, in terms of resistance to acidic treatment and lack of reducing moieties.

In 1903, in Vienna, the Austrian biologist Franz Schardinger isolated the strain of bacteria responsible for the formation of the crystalline products described by Villiers. He distinguished two types of polysaccharides by performing an iodine colorimetric test. He named these two types crystalline dextrin A and crystalline dextrin B (now known as α - and β -cyclodextrins). Freudenberg and Jacobi in 1935 discovered the existence of larger dextrins called γ -dextrin.

Researches on dextrins were continued by Hans Pringsheim, a German chemist and biochemist.^{13,14} The main achievement of his work was the discovery that CDs were able to form inclusion compounds with organic guests, a characteristic that continues to keep this class of polysaccharides being widely used.¹⁵ In 1936, Freudenberg hypothesized that dextrins have a cyclic structure composed of glucose units bound together by α -(1 \rightarrow 4) glycosidic linkages.¹⁶ Few years later, in 1954, Cramer published a book entitled “Inclusion compounds” where he summarized the structural and physico-chemical characteristics of α -, β - and γ -CDs.¹⁷ From the 1970s the modern studies on CDs began with research works of Szejtli in Hungary and Osa in Japan.

1.1.2. Structural and physico-chemical characteristics of cyclodextrins

CDs are cyclic oligomers of glucose, bound via α -(1 \rightarrow 4) glycosidic linkages. They are composed of 6, 7 or 8 D-glucopyranose units, corresponding to α -, β - and γ -CD, respectively, as illustrated in Figure 1.1.

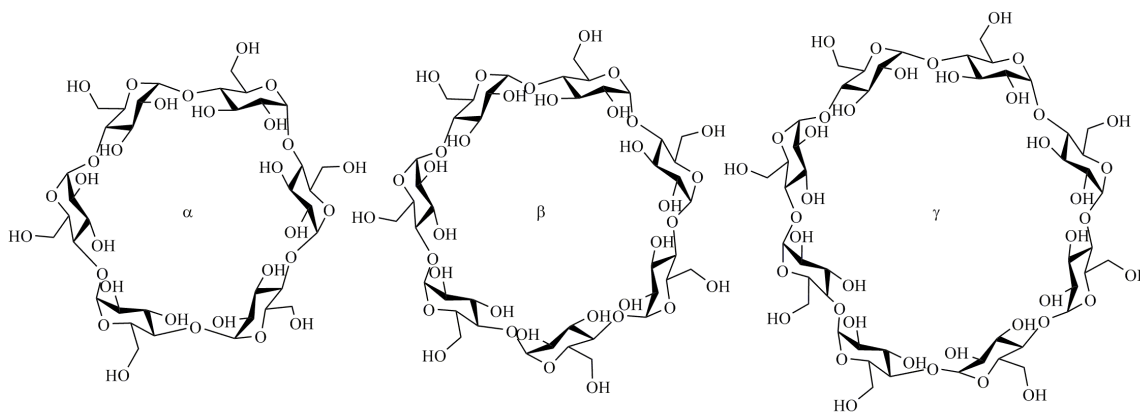


Figure 1.1: Chemical structures of α , β and γ -CDs

From the crystal structure of CD derivatives could be observed that all glucose residues in the torus-like ring have the thermodynamically favoured chair conformation because all substituents are in equatorial position. They possess the primary hydroxyl groups at the primary rim of the macrocycle and the secondary hydroxyl groups at the secondary rim, as illustrated in Figure 1.2. The differences of chemical reactivity of the primary alcohol functions and the secondary alcohols represents an attractive feature of this class of molecules, as it allows fairly easy regio (rim)-selective chemical modifications of the macrocycles. The main structural characteristics of α -, β - and γ -CD are summarized in (Table 1.1).

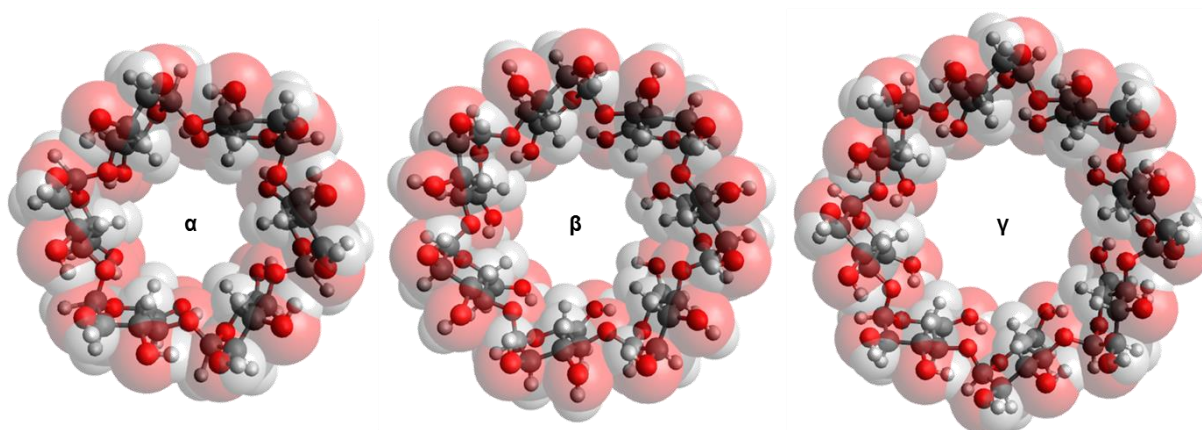


Figure 1.2: X-ray crystal structure of α -, β - and α -CD, water molecules are omitted for clarity (from the X-ray crystal structure published by Lindner and Saenger.18)

Table 1.1: physicochemical properties of three cyclodextrins derivatives¹⁹

	α -CD	β -CD	γ -CD
Number of glucose unit	6	7	8
Molecular weight (g/mol)	972	1135	1297
Internal diameter (Å)	4.7-5.2	6.0-6.4	7.5-8.3
External diameter (Å)	14.2-15.0	15.0-15.8	17.1-17.9
Depth (Å)	7.9-8.0	7.9-8.0	7.9-8.0
Internal cavity volume (Å ³)	174	262	472
Solubility in water (25°C, g/L)	145	18.5	232
Number of H ₂ O molecules in the cavity	6	11	17
Melting point (°C)	250-260	255-265	240-245
pK at 25°C	12.332	12.202	12.081

The primary and secondary hydroxyl groups at the primary and secondary rim of CDs ensure their good water solubility with values of 145, 18.5 and 232 g L⁻¹ at 25°C for α -, β - and γ -CD, respectively. The lower water solubility of the β -CD compared to α - and γ -CD is due to the geometry of the macrocycle. β -CD structure favors the formation of a set of hydrogen bonds linking the hydroxyl groups together at the lower rim of the macrocycle, therefore limiting their ability to interact with the surrounding water molecules. The water solubility of CDs in addition to their hydrophobic cavity of 174, 262 and 427 Å³ for α -, β - and γ -CD, respectively, makes this class of molecule an excellent candidate receptor for supramolecular host-guest chemistry. Hereinafter, we will briefly describe the host-guest inclusion properties of CDs.²⁰ CDs can also be used to form asymmetric inclusion complexes. Indeed as CDs are chiral macrocycles they are largely exploited to produce chiral sensors²¹ and chiral stationary phases in chromatography.²²⁻²⁶

1.1.3. Industrial production of cyclodextrins

CDs are produced via enzymatic conversion of starch or starch derivatives by CD glucosyltransferase (CGTase, EC 2.4.1.19).²⁷⁻²⁹ CGTases are produced by various bacterial species such as *B. macerans*,^{19,28} *B. stearothersophilus*,^{28,30} *B. circulans*^{30,31} and *K. oxytoca*.³² The two main production processes of CDs are the “solvent-” and “non-solvent” processes; the current industrial production of CDs is primarily based on the solvent process, as illustrated in Figure 1.3.

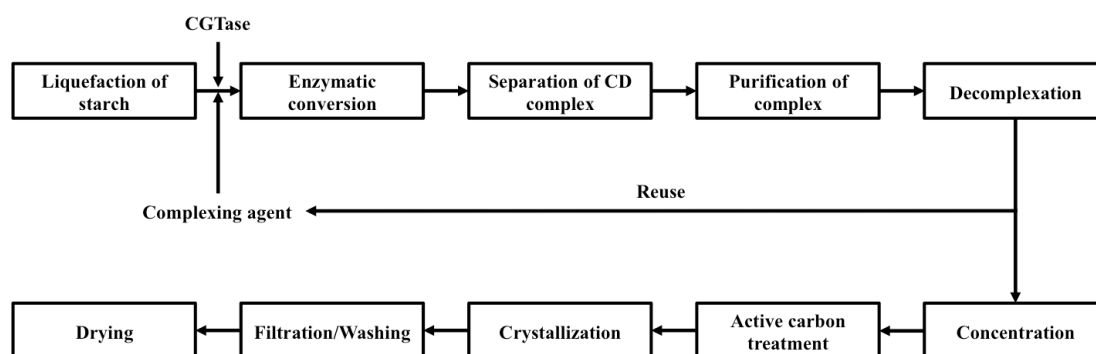


Figure 1.3: Diagram of solvent processes for industrial production of CDs³³ (Reproduced with permission from Ref.33 © Elsevier, 1996.)

The solvent process begins with starch liquefaction followed by subsequent jet cooling. The starch solution is thus cooled down to the optimum temperature and CGTase is then added to start the enzymatic conversion. The use of organic additives that causes CD precipitation, leads to a tremendous enhancement of the enzymatic conversion process via equilibrium displacement. In other words, the decrease of CD concentration would drive the equilibrium towards CD production. The size of the CDs synthesized following this method is strongly dependent on the choice of the enzyme and the additives used. Subsequently, the CDs are separated and purified from the reaction mixture by centrifugation or filtration, followed by washing. The organic additives are removed by suspending and heating the CDs in aqueous solution followed by distillation or extraction. The product mixture is then concentrated and treated with activated carbon. Eventually, CDs are isolated by crystallization and filtration.^{28,33,34}

The non-solvent process (Figure 1.4) is mainly used for the production of β -CD, which, due to its differential solubility, can be easily purified by crystallization.^{33,35} The purification of α - and γ -CDs according to this process is costly, and typically results in low yields and a high range of by-products. The advantage of this process is that the product can be used in the food industry without restriction because of the absence of organic additives.

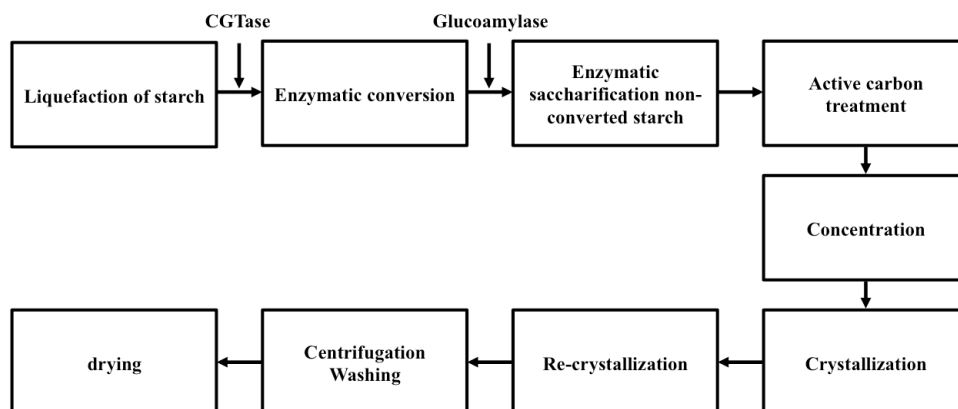


Figure 1.4: Diagram of non-solvent processes for industrial production of β -CDs³³ (Reproduced with permission from Ref.33 © Elsevier, 1996.)

1.1.4. Formation of host-guest inclusion compounds

One of the most interesting characteristics of CDs is their ability to form inclusion complexes with a large variety of organic guest molecules in solution.²⁰ Those complexes are formed by the partial inclusion of the guest molecules inside the hydrophobic cavity of the CD macrocycle, as shown in Figure 1.5.

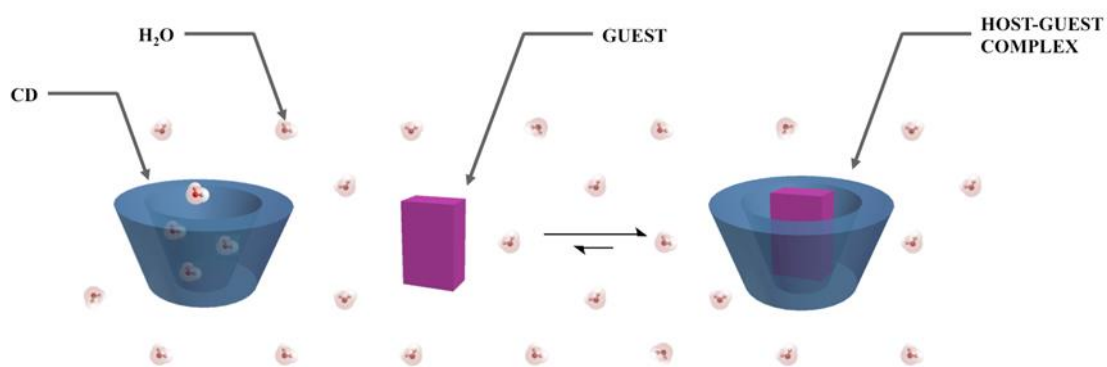
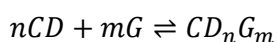


Figure 1.5: inclusion complex of a hydrophobic guest molecule and a CD in water

Water molecules occupy the CDs cavity under aqueous conditions, but the interactions between water and the interior of the macrocycle are weak and the system is consequently energetically not favourable. The presence of a guest molecule in solution with poor polarity leads to the formation of an inclusion complex, wherein the guest molecule replaces the bound water molecules with the condition that the geometry of the guest molecule is compatible with the internal space of the host CD. The complexation of CDs with guest (G)

entities can be described by a binding equilibrium model and the association constant of the complex can be defined as shown in Equation 1.1:



$$K_a = \frac{[G_m][CD_n]}{[G]^m[CD]^n} \quad \text{Equation 1.1}$$

They are different driving forces for the complex formation. For instance, the release of water molecules from the cavity leads to an increase in entropy ($\Delta S_{complex}$) of the system. Additionally, van der Waals forces between guest and cavity of CDs contribute to complex formation. In some systems, hydrogen bonding is also taking place between guest and the hydroxyl groups at the primary and/or secondary rims of CDs.

2D NMR spectroscopy can be used for the study of inclusion complex formation in solution.^{36,37} The presence of a guest molecule inside the cavity typically induces changes in the spectral properties of both the host and the guest, allowing for a structural characterization of the complex. Single crystal X-ray crystallography technique can be used to study the crystal structure of inclusion complexes in the solid state.³⁸ However, the production of crystals of sufficient quality for X-ray diffraction is often challenging. A number of additional characterization techniques have been applied to study the formation of complexes. These include thermogravimetric methods, polarimetry, infrared, fluorescence, UV-visible, and electron paramagnetic resonance spectroscopies, to name but a few.³⁹

1.2. Multivalency

The term multivalency is defined as simultaneous non-covalent binding of m -valent receptors and n -valent ligands ($m, n > 1$). Multivalent interactions, in contrast to monovalent interactions, have the advantage of a multiple and therefore radically enhanced binding strength on a molecular scale; *cf.* Figure 1.6. The simultaneous binding of multiple recognition sites of one molecule to the recognition sites of another results in a higher binding strength than the sum of the corresponding monovalent interactions.¹

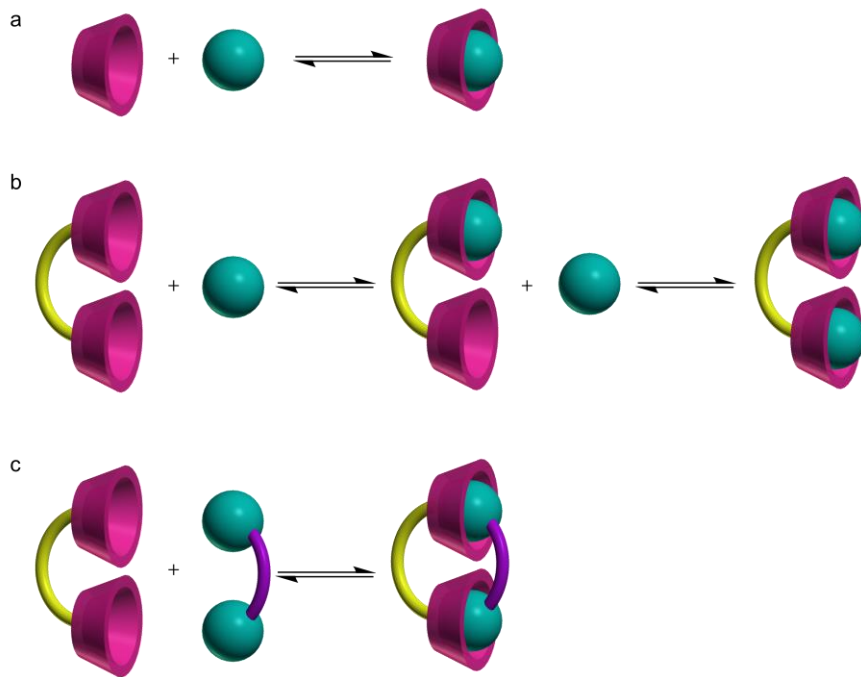


Figure 1.6: Schematic representation of a) monovalent interactions, b) multiple monovalent interactions and c) multivalent interactions

In order to better understand the distinct contributions of each multivalent molecule toward enhancement in binding affinity, it is important to understand the governing thermodynamic principles of multivalency.

1.2.1. Thermodynamic principles of multivalent interactions

In a monovalent system, the free enthalpy (ΔG_{mono}) can be calculated from the difference of enthalpies in bound and unbound states. However, this duality is no longer applicable in multivalent systems. Indeed, for an n -valent receptor distinguished by the number j of occupied receptors, $n+1$ different binding state exists. Therefore in order to calculate the free binding enthalpy of a multivalent system (ΔG_{multi}), it has to be considered which binding states ($0 < j < n$) is considered as bound or unbound. The probabilities for j receptor sites to bind an n -valent receptor can be defined by following formulas (Equation 1.2):

$$\binom{n}{j} = \frac{n!}{(n-j)!j!} \quad \text{Equation 1.2}$$

This assignment is critical for the probable cooperative effect of multivalent bindings.⁴⁰ Cooperativity take place when binding of one ligand to a receptor affects the binding of additional ligands to that receptor. ΔG_{multi} can be related to that of N monovalent interactions ($N\Delta G_{mono}$) and the degree of cooperativity can be defined as shown in Equation 1.3.

$$\alpha = \text{cooperativity} = \frac{\Delta G_{\text{multi}}}{N\Delta G_{\text{mono}}} \quad \text{Equation 1.3}$$

Cooperativity can be classified as (i) positively cooperative ($\alpha > 1$), when the subsequent binding of another ligand to a receptor has a higher probability than that of previous one (ii) non-cooperative or additive ($\alpha = 1$), when the binding probability is identical and (iii) negatively cooperative or interfering ($\alpha < 1$), when the binding probability is lower.

Cloninger and co-workers defined the cooperativity factor (α) for estimating the magnitude of multivalent associations relative to monovalent bindings. They studied the multivalent binding of carbohydrate-functionalized dendrimers to the lectin Concanavalin A.⁴¹ They calculated the level of multivalent interactions as shown in Equation 1.4.

$$K_N^{\text{poly}} = (K^{\text{mono}})^{\alpha N} \quad \text{Equation 1.4}$$

where N represent the number of receptor-ligand interactions. They demonstrated that multivalent affinities could be influenced in predictable ways.^{42,43}

In order to assess multivalent binding effects, Whitesides and co-workers defined the enhancement factor (β).⁴⁴ They assigned the influence of multivalent associations relative to the monovalent association, as the ratio of avidity to monovalent affinity constant as shown in Equation 1.5. Avidity of a multivalent interaction is defined as the dissociation constant of the completely associated receptor-ligand complex with N receptor-ligand interactions relative to completely dissociated forms of the multivalent receptor-ligand complex.

$$\beta = \frac{KN_{\text{multi}}}{k_{\text{mono}}} \quad \text{Equation 1.5}$$

where N , represent the theoretical number of receptor-ligand. The enhancement factor (β) reflects the strength of a multivalent association relative to a monovalent association. However, this enhancement factor has the disadvantage that it simultaneously includes the influence of cooperativity and symmetry effects. The symmetry factor of equilibrium can be calculated based on the symmetry number of the molecules involved in the reaction. The symmetry number of a molecule (σ) is defined as the number of equivalent positions a molecule can be turned into via a simple rotation around an axis or axes. The symmetry number influences the entropy of a molecule by a factor of $-R \ln \sigma$. As a result, for an equilibrium $A + bB \rightleftharpoons cC$, if the symmetry number of A, B and C are σ_A , σ_B and σ_C respectively, the effect of their symmetry on the equilibrium constant is given by the factor $\sigma_A^a \sigma_B^b / \sigma_C^c$.

Bundle developed a thermodynamic model for designing multivalent ligands demonstrating maximal avidity enhancement.⁴⁵ Based on this approach, the avidity enhancement of a multivalent binding is dependent of three different components (i) the free energy change for the first receptor-ligand interaction (ΔG°_{inter}); (ii) free energy change for each additional interaction in the multivalent complex (ΔG°_{intra}); (iii) a combinatorial factor reflecting the probability of association and dissociation of individual ligands (Ω_i) (Equation 1.6)

$$\Delta G^\circ_{avidity} = \Delta G^\circ_{inter} + \Delta G^\circ_{intra} \sum_{i=1}^{i_{max}} w_i (i - 1) + RT \sum_{i=1}^{i_{max}} w_i \ln\left(\frac{w_i}{\Omega_i}\right) \quad \text{Equation 1.6}$$

w_i is a weight coefficient which takes into account the distribution of bound species at equilibrium. Based on this model, Kitov and Bundel developed a system using oligovalent carbohydrate inhibitors and different scaffold topologies.⁴⁵ They observed an increase in affinity with radial topology compared to linear, circular and indifferent topologies (Figure 1.7) for tailored multivalent ligand-receptor, which was attributed to intramolecular binding and avidity entropy.

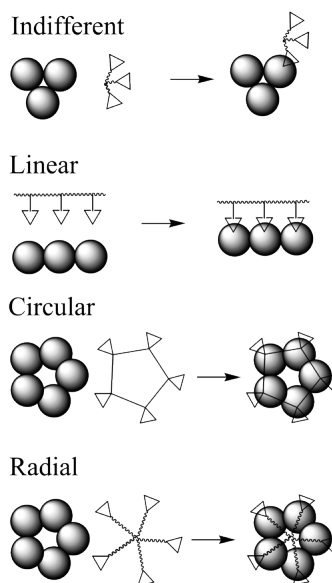


Figure 1.7: Schematic representation of different topologies of multivalent interactions (Reproduced with permission from Ref.45. © American Chemical Society, 2003.)

Another important factor in the mechanism of multivalent binding is the influence of the statistical rebinding of multivalent ligands to multivalent receptors. A term that is important for assessment of this statistical rebinding is defined as effective concentration. Effective concentration represents a probability of interaction between two reactive or complementary interlinked entities. The concept of effective concentration originates from

the field of polymer chemistry where it was introduced for the estimation of the kinetics and thermodynamics of cyclization reaction for intramolecular reaction in polymer synthesis.⁴⁶ Similarly, effective concentration (C_{eff}) can be used for the assessment of the multivalent interactions. The first interaction of a multivalent ligand with a multivalent receptor alters the ligand site concentration as experienced by the neighbouring free receptor site. If this so-called effective concentration is higher than the actual receptor concentration in solution, intramolecular (multivalent) binding is favoured. If the ligand site concentration in solution is higher than C_{eff} experienced by the receptor site, the binding will most likely proceed in an intermolecular fashion.

The association constant for the n -valent interaction (K_n) for a multivalent ligand-receptor system is defined by Equation 1.7.²

$$K_n = bK_i C_{eff}^{n-1} \quad \text{Equation 1.7}$$

Here, n is valency of the ligand, b is a scaling factor incorporating statistical factors determining the numbers of possible association and dissociation paths in the subsequent interaction steps and K_i is intrinsic association constant.

Theoretically C_{eff} is similar to effective molarity (EM). In those cases where the multivalent interaction is involved of multiple non-cooperative interactions, C_{eff} equals EM . However, C_{eff} is based on concentrations estimated from physical geometries of complexes while EM is represented as the ratio of intra- and intermolecular association constants. Reinhoudt extend EM definition to higher-order systems and developed a model to predict the EM based on the valency of the ligands (n). EM can be given by Equation 1.8 for an intermolecular n -valent interaction with an association constant K_n .

$$EM = \left(\frac{K_n}{b k_i} \right)^{\left(\frac{1}{n-1} \right)} \quad \text{Equation 1.8}$$

The dissociation rate of a multivalent ligand is only dependent on the concentration of the monovalently bound entities. For an intramolecular multivalent interaction, the concentration of the monovalently bound entities is dependent on the EM . That suggests that it is possible to make complexes based on multivalent interactions that combine high avidity with the possibility of kinetic control and reversibility.⁴⁷

1.2.2. Multivalency in solution

In this section we describe several important studies that are performed on different multivalent systems in solution.

1.2.2.1. Zinc porphyrin-pyridyl motif

The coordination of pyridyl bases to zinc porphyrins is one of the examples of the supramolecular systems that highlighted the importance of molecular design in multivalent systems.⁴⁸ Anderson *et al.* studied the supramolecular interactions between a series of rigid and linear porphyrin dimers, trimers and tetramers with a series of rigid and flexible multivalent pyridyl bases. They demonstrated that an appropriate molecular design can result in very efficient multivalent bindings.⁴⁹ Indeed, the association between a bis(Zn porphyrins) as a host and 3,3'-bipyridine as a guest gave a binding enhancement of 3×10^5 compared to the corresponding monovalent interaction (Figure 1.8). This enhancement is attributed to the conformational preorganization of bis(Zn porphyrins). The *EM* of this system was 76 M. The high *EM* is due to the high complementarities between the rigid hosts and guests resulting in a perfect fit between receptors and ligands. For comparison, the interaction between the corresponding linear zinc-porphyrin dimer with some rotational freedom around the central butadiyne bond as a host and 3,3'-bipyridine as a guest was studied. The *EM* of this system was 0.5 M. Nevertheless, one has to consider that beside all advantages of conformational preorganization, an imperfect design at the angstrom scale may lead to steric hindrance and weak binding.

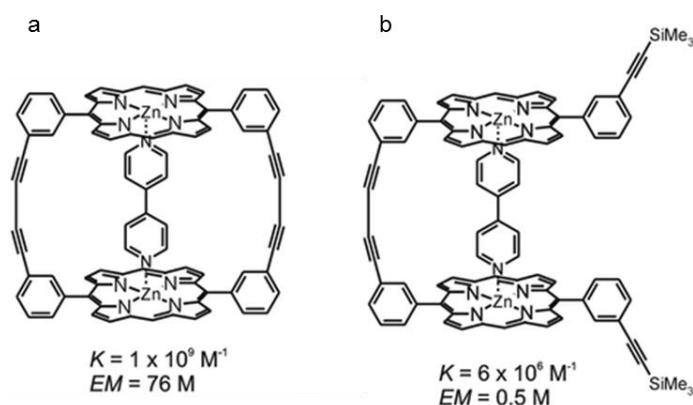


Figure 1.8: examples of multivalent systems using zinc-porphyrin-pyridyl system; a) the pre-organized host; b) using a linear bis(Zn porphyrin) which is less pre-organized (Reproduced with permission from Ref.49. © Royal Society of Chemistry, 1995.)

1.2.2.2. Pseudorotaxanes

Stoddart and co-workers used pseudorotaxanes from crown ethers and ammonium-based cation as hosts and guests in a multivalent system (Figure 1.9).⁵⁰ They demonstrated that the trivalent interaction between a triphenylene-based tris(crown ether) and the tris(dibenzylammonium) trication has an association constant of 10^6 M^{-1} in acetonitrile. This corresponds to a binding enhancement of 10^4 compared to the corresponding monovalent interaction between single crown ether and a single cation.

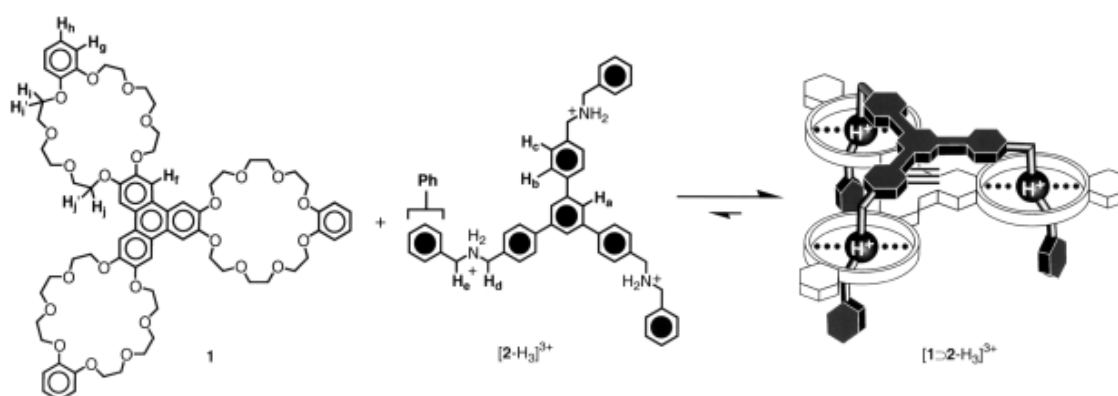


Figure 1.9: The trivalent equilibrium interaction between tris(crown ether) and the tris-ammonium ion (Reproduced with permission from Ref.50. © John Wiley and Sons, 2003.)

The assessment of this multivalent system revealed that the trivalent complex could be dissociated by deprotonation of the ammonium cations after addition of suitable bases or DMSO, which competes with the crown ether oxygen in hydrogen bonding of ammonium cations. The dissociation mechanism of the system upon addition of DMSO was monitored using NMR. The results revealed a stepwise dissociation process in which the trivalent complex gradually dissociated through the divalently and monovalently bound states (Figure 1.10).

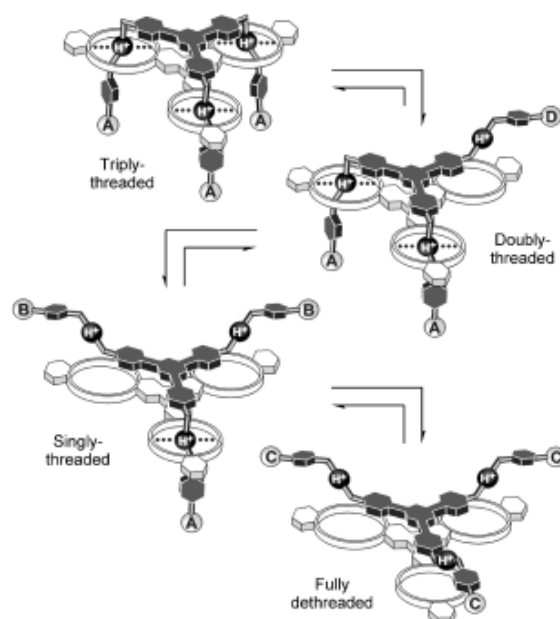


Figure 1.10: A schematic representation of the equilibration supramolecular interaction between the tris-crown ether and the tris-ammonium ion, involving entities that are triply-, doubly-, and singly-bound, as well as free (Reproduced with permission from Ref.50. © John Wiley and Sons, 2003.)

1.2.2.3. Vancomycin-D-alanine-D-alanine

Whitesides and Rao studied multivalent interaction of vancomycin and D-alanine-D-alanine ($^D\text{Ala}^D\text{Ala}$).^{51,52} Vancomycin can form five hydrogen bonds with $^D\text{Ala}^D\text{Ala}$ as shown in Figure 1. They demonstrated that a trivalent derivative of vancomycin binds a $^D\text{Ala}^D\text{Ala}$ trimer with an association constant of $2.2 \times 10^{16} \text{ M}^{-1}$. This multivalent interaction is 4×10^{10} times stronger than the corresponding monovalent interaction (Figure 1.11).

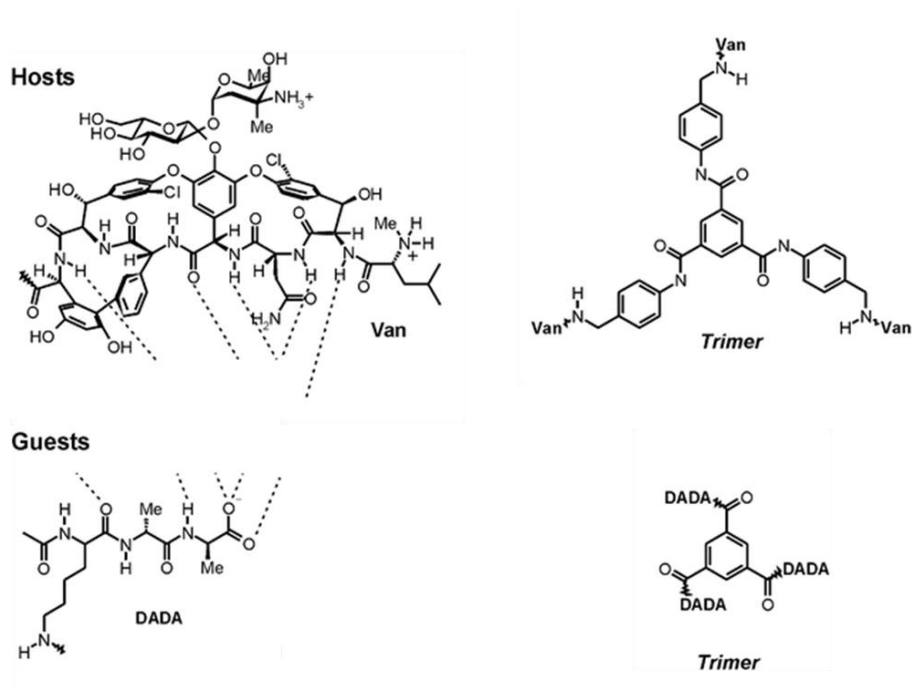


Figure 1.11: Multivalent host (trivalent vancomycin) and guest (^DAla^DAla trimer) entities (Reproduced with permission from Ref.64. © American Chemical Society, 2000.)

Very slow dissociation kinetics for the multivalent complex formed in water was measured. Indeed, based on the binding constant and diffusion limited association rate ($k_{on} = 1 \times 10^9$; $M^{-1} s^{-1}$) they estimated a minimum dissociation rate of $k_{off} = 4 \times 10^{-8}$; $M^{-1} s^{-1}$ in water, which corresponds to a half-life of 200 days. The dissociation could be drastically speed up by using competitive monovalent ^DAla^DAla. Indeed, in the presence of 86 mM monovalent ^DAla^DAla, 40% of the trivalent supramolecular complex was dissociated after 45 min. A faster dissociation could be achieved by using concentrations of monovalent ^DAla^DAla that are higher than the effective molarity.

1.2.2.4. Cyclodextrins host-guest complexes

Reinhardt and co-workers demonstrated that the enhancement of the affinity of CD dimers for multivalent guests can be explained in a quantitative sense based on multivalency (Figure 1.12).⁵³ They demonstrated that the multivalent interaction between a CD host dimer and a bis(adamantane) guest exhibit an association constant of $10^7 M^{-1}$. That corresponds to an enhancement factor of 200 over the analogous monovalent system. Based on calorimetric measurements, it was also demonstrated that the enthalpy of binding for the multivalent interaction was twice lower ($-14.8 \text{ kcal mol}^{-1}$) than the corresponding monovalent

interaction ($-7.0 \text{ kcal mol}^{-1}$), which indicates an increase in the stability of the multivalent system.

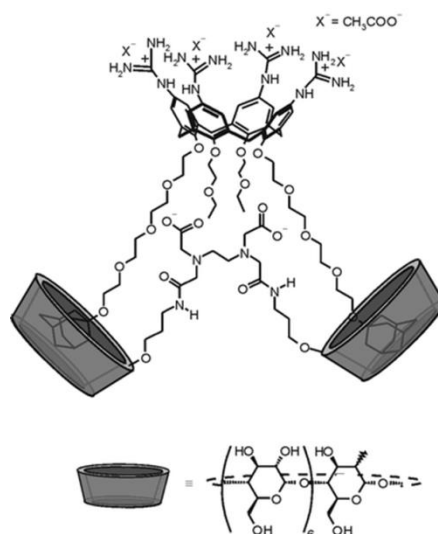


Figure 1.12: Multivalent interaction of a β -CD dimer as a host and a bis(adamantyl) guest (Reproduced with permission from Ref.53. © American Chemical Society, 2004.)

Petter and co-workers, studied the supramolecular binding of toluidino-2-naphthalene sulfonate with β -CD dimers tethered by spacers of variable length (Figure 1.13).⁵⁴ They demonstrated a linear relation between binding affinity and invers cubic tether length that can be explained in terms of effective concentration. Indeed, the linear trend of binding affinity for a guest entity versus spacer length of a CD dimer was observed for several different CD dimer systems.⁵⁵⁻⁵⁷

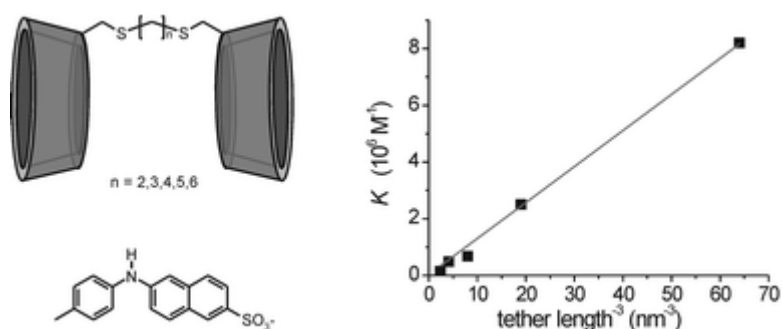


Figure 1.13: Left, multivalent host (β -CD dimers tethered) and guest (toluidino-2-naphthalene sulfonate) entities; right, the plot of binding affinity versus invers cubic tether length for complexation of the toluidino-2-naphthalene sulfonate and CD dimer with variable tether length (Reproduced with permission from Ref.2. © Royal Society of Chemistry, 2004.)

Breslow *et al.* demonstrated that also for CD dimers, the rigidity in both host and guest can result in higher binding affinities compared to their monovalent analogues.^{58,59} Nevertheless, an exact compatibility is needed in such a system. Indeed, mismatches in rigid systems can

result in low effective concentrations and therefore inefficient multivalent binding. Based on this phenomenon, Reinhoudt and co-workers developed β -CD dimers with photo-switchable binding properties.⁶⁰⁻⁶² They synthesized β -CD dimers that were tethered via photo-switchable diarylethene spacers that could be reversibly switched between a flexible and more rigid state. They demonstrated that the stability constant found for the binding of meso-tetrakis(4-sulfonatophenyl)porphyrin by the open form of the β -CD dimer, is a factor 35 higher compared to the binding of the close form of this dimer. This difference allowed for a controlled, reversible release and uptake of the multivalent guest by the β -CD dimers as hosts (Figure 1.14).

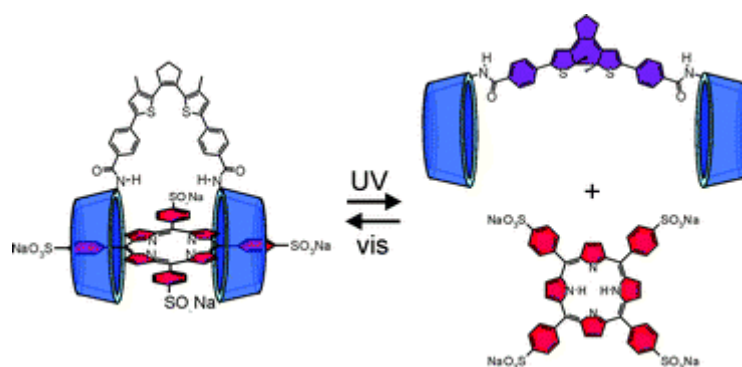


Figure 1.14: A schematic representation of the photo-switchable supramolecular interaction between a β -CD dimers and multivalent porphyrin guest (Reproduced with permission from Ref.61. © Royal Society of Chemistry, 2004.)

1.2.3. Multivalency at interfaces

Multivalent interactions can be applied for a strengthening of an interaction between different interfaces. A systematic assessment concerning multivalency, effective concentration and the effect of competitive functionalities on the dissociation rate of multivalent complexes can be achieved by varying structure, density and environment of the immobilized functionalities at interfaces.

1.2.3.1. Cyclodextrin-based surfaces

CDs have been widely studied as molecular building blocks in design of functional surfaces and interfaces because of their outstanding molecular recognition properties. CDs do not possess an intrinsic ability to self-assemble at interfaces or to bind covalently to surfaces. Nevertheless, a series of rational chemical modifications of the CD macrocycle have proven successful in the production of CDs that can react covalently with surfaces and form self-assembled monolayers (SAMs).⁶³ SAMs of appropriately modified CDs were successfully

prepared on gold or silicon dioxide surfaces and showed to retain their molecular recognition/inclusion properties.^{63,64}

The design of CDs that can form SAMs on gold typically requires the introduction of thiol or thioether functionalities in the CD structure; chemical structures of some selected β -CD SAMs building blocks such as *per*-thio- β -CD (**1**), thioether-bearing CDs (**2**, **4**) and thiol derivative of β -CD (**3**) are given in Figure 1.15.

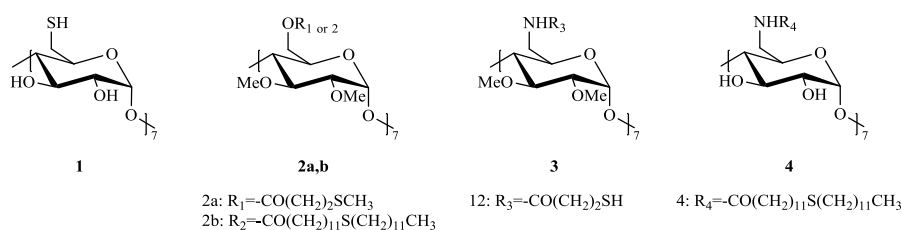


Figure 1.15: chemical structure of some selective β -CD SAMs building blocks

For the first time in 1995, Rojas *et al.* reported the formation of CD-based SAMs on gold.⁶⁴ The proof of principle that the immobilized CDs retained their molecular recognition properties was established, as effective binding for ferrocene (Fc) and *m*-toluic acid was shown.⁶⁴ Nelles *et al.* studied SAMs of mono- and multi-thiolated derivatives of β -CD with different chain lengths on gold surfaces.⁶⁵ It was demonstrated that the orientation of the CD cavities could be controlled by varying either the number of thiol groups per CD molecule or the length of the alkyl chains. Beulen *et al.* studied SAMs of a thioether derivative of β -CD (**2**).⁶⁶ Those SAMs were reported to have more attachment points to the surface as compared with thiol-based β -CDs; the SAMs produced showed higher molecular densities and stabilities. Shahgaldian *et al.* used the same CD to coat a surface plasmon resonance (SPR) sensor and demonstrated that the produced SAMs possess the enantioselective binding properties of a thyroid hormone, namely thyroxine.⁶⁷

SAMs of CDs have also been prepared on SiO₂ surfaces. For example, Onclin *et al.* immobilized a *per*-amino derivative of β -CD (NH-CD) on a SiO₂ surface.⁶⁸ In order to introduce amino groups on the SiO₂ surface, first monolayers of undecyl isocyanide were produced by reacting the bare SiO₂ surface with 1-cyano-11-trichloro-silylundecane. The isocyanide functions were consecutively reduced to the corresponding amino groups using

sodium bis(2-methoxyethoxy)aluminiumhydride. The final step consisted of introducing functional isothiocyanate onto the monolayer, this was achieved by using 1,4-phenylene diisothiocyanate, as shown in Figure 1.16. The SAM layers formed were reacted with the *per*-amino-CD (NH-CD) to allow its covalent immobilization. It was demonstrated that the quality of these layers, in terms of molecular packing and the orientation of β -CDs, was similar to that of immobilized β -CD monolayers on a gold surface. The inclusion of fluorescent guest molecules on such a modified silicon oxide surface was visualized by confocal microscopy; this was not possible for SAMs on gold substrates owing to the fluorescence quenching effects of the metal. Molecular patterns of labelled guest-functionalized molecules were printed by micro-contact printing (μ CP) on SAMs of the β -CD derivatives.

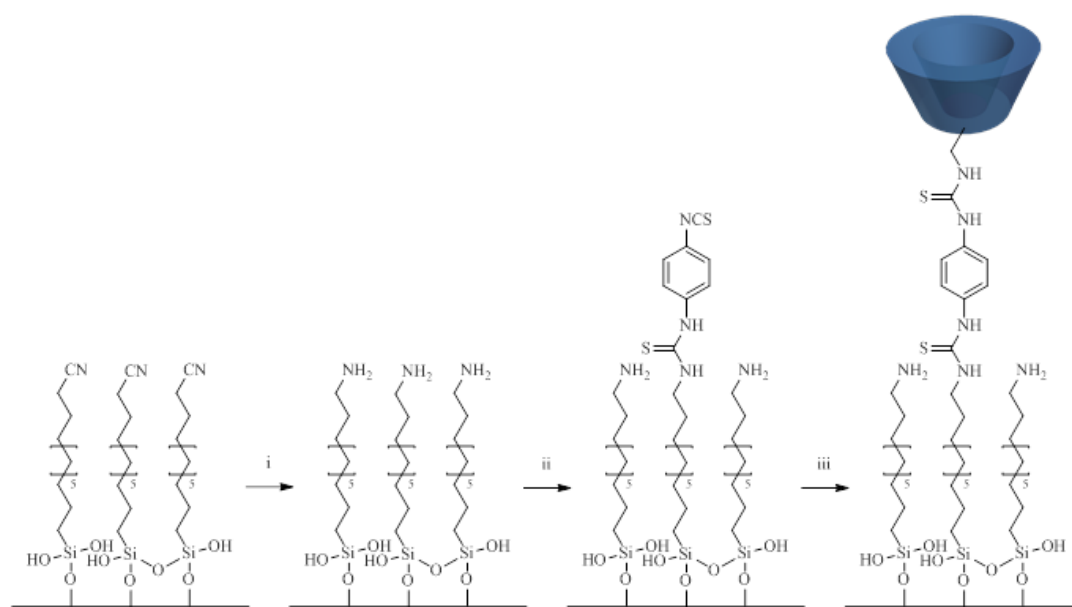


Figure 1.16: Formation of an organized monolayer of an amino derivative of β -CD (5) on a silicon oxide surface. i) sodium bis(2-methoxyethoxy)aluminiumhydride; ii) 1,4-phenylene diisothiocyanate; iii) NH-CD

Auletta *et al.* demonstrated the ability of CD-based SAMs on SiO_2 to bind, in a reversible manner, to adamantyl- or ferrocenyl-labelled guest molecules.⁶⁹ The binding properties of the guest molecules to these surfaces, in terms of transfer and pattern stability, were demonstrated to be similar to that of immobilized β -CD monolayers on gold. It was also demonstrated that rinsing the substrate with buffer or water did not affect the patterns formed, while rinsing with a solution of competitor hosts (soluble β -CD) resulted in the release of the guest molecules from the surface.

1.2.3.1.1 Molecular printboards of CDs

In 2002, Reinhoudt defined the term “molecular printboard” as an immobilized monolayer of host molecules on a solid substrate onto which multivalent guest molecules can be positioned in a controlled and reversible manner.⁷⁰ The whole concept of molecular printboards relies on multivalency. CD-based molecular printboards were developed by Reinhoudt using SAMs of CDs as “host surfaces” and guest molecules possessing at least two chemical moieties that are known to form inclusion complexes with CDs.⁷¹ These molecular printboards were used as platforms for the precise positioning of multivalent guest molecules using micro-contact printing (μ CP)^{68,72-74} and nanolithography.^{69,75} For example, defined circular patterns of ferrocenyl-functionalized dendrimers (multivalent guest molecules) were transferred onto a β -CD modified substrate using μ CP.¹¹ The stability of the complexes formed was demonstrated in water by solely removing the non-specifically bound molecules during a thorough rinsing of the monolayer. However, local electrochemical conversion of Fc to Fc^+ , achieved using a scanning electrochemical microscopy, caused a local release of the surface-bound molecules, owing to the lower affinity of CDs for the ionic ferrocene species, as displayed in Figure 1.17.

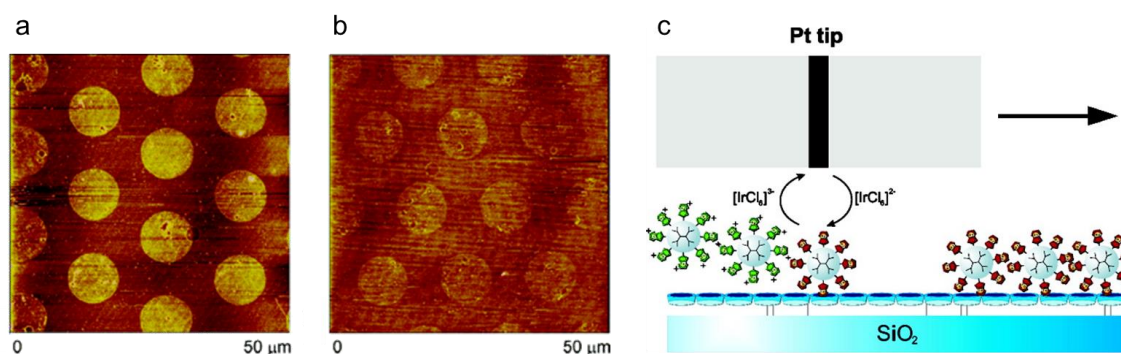


Figure 1.17: Atomic force microscopy images of the μ CP Fc-functionalized dendrimers patterns at β -CD SAMs on glass substrates a) before rinsing; b) after rinsing with water; c) schematic representation of induced electrochemical desorption of guest molecules from molecular printboards using scanning electrochemical microscopy (Reproduced with permission from Ref.11. © American Chemical Society, 2006.)

Recently, Yang *et al.* demonstrated that ferrocene-tagged yellow fluorescent proteins (Fc-YFPs) could be attached in an oriented, reversible fashion to β -CD molecular printboards, as shown in Figure 1.18.⁷⁶ It was shown that a covalent disulfide bond between two YFP proteins resulted in a switch from monovalent to divalent ferrocene, which resulted in more stable protein immobilization. Fc-YFPs could be patterned on β -CD SAMs as uniform layers.

Repetitive adsorption and desorption cycles were interchangeable upon electrochemical reduction and oxidation.

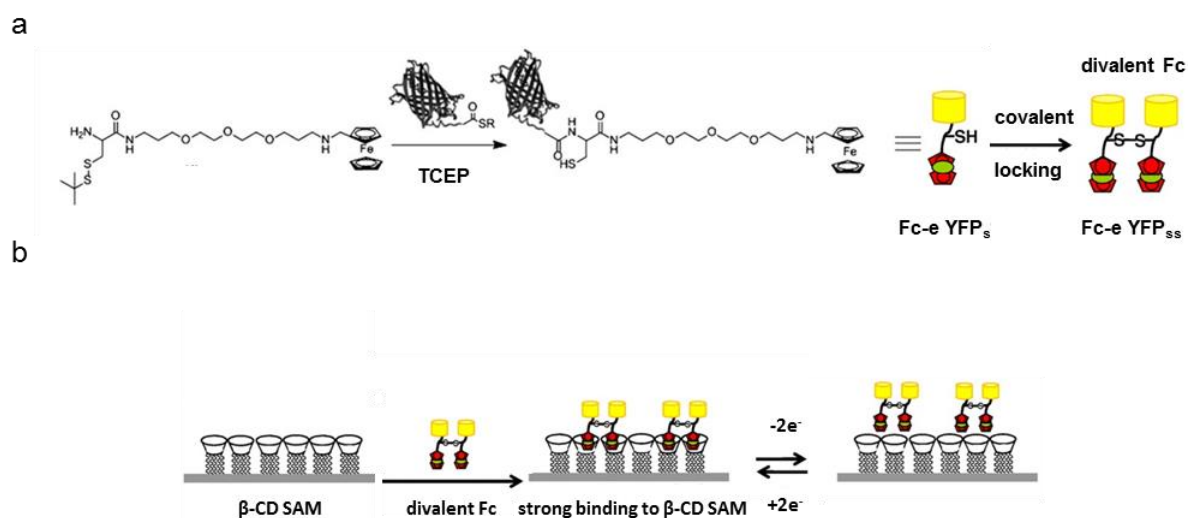


Figure 1.18: Schematic representation of a) conjugation of cysteine-functionalized Fcs and thioester-functionalized yellow fluorescent proteins; followed by covalent locking of two Fc-YFPs; b) immobilization of divalent Fc-YFPs onto thioether-functionalized β -CD monolayers (Reproduced with permission from Ref.76. © American Chemical Society, 2012.)

A similar strategy was used for the fabrication of enzymatically functionalized microfluidic systems. It was demonstrated that a reusable homogeneous enzyme layers could be formed on micro-channels. This was achieved by formation of β -CD-adamantane and biotin-Streptavidin (SAv) supramolecular interactions; *cf.* Figure 1.19. The specific immobilization of an alkaline phosphatase (AlkPh) onto the β -CD molecular printboards was studied using a surface plasmon resonance (SPR) flow cells. A step-wise assembly process was performed; first β -CDs modified gold substrates were functionalized by a biotinylated bisadamantyl linker (**6**). Subsequently in order to minimize the non-specific protein adsorption, an ethylene glycol based mono-adamantyl linker (**5**) was also immobilized at the surfaces. Successively, SAv was attached to the surface via site-specific avidin-biotin interactions. As a final step, biotinylated alkaline phosphatase (bt-AlkPh) (**8**) was immobilized at the SAv modified substrates. It was demonstrated that the structure and activity of the immobilized enzyme was retained.⁷⁷

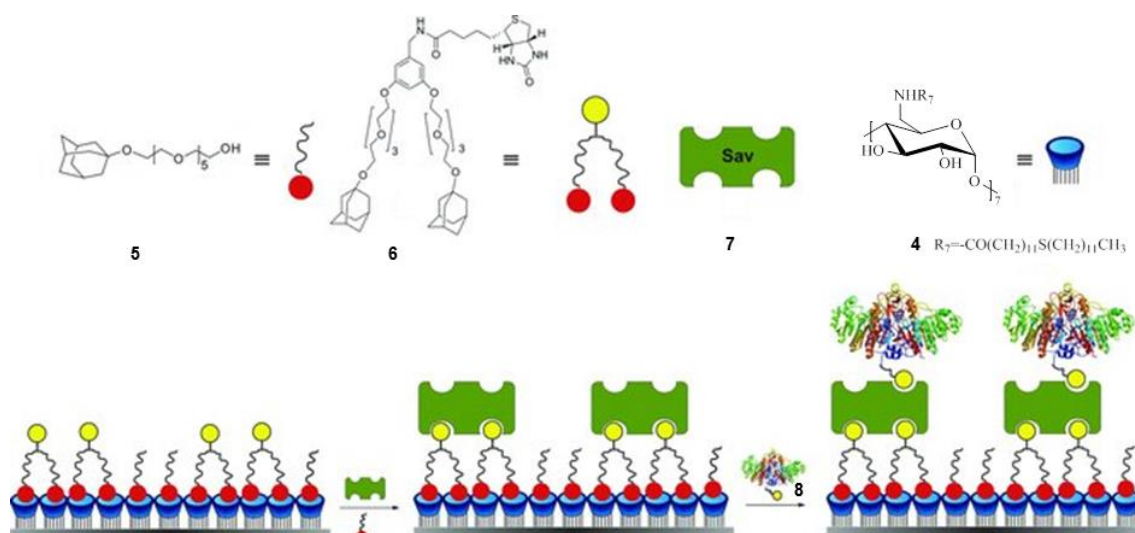


Figure 1.19: Schematic representation of the chemical structures of the building blocks and scheme for the step-wise assembly process (Reproduced with permission from Ref.77. © John Wiley and Sons, 2012.)

González-Campo *et al.* recently published a versatile surface modification method based on CD molecular printboards.⁷⁸ Alkyne-terminated coumarin monolayers were used to chemically attach a *per*-azido- β -CD through a Cu(I) catalysed “click” reaction. The resulting CD SAM surfaces were further functionalized through supramolecular μ CP and by reactive μ CP-induced click chemistry, as illustrated in Figure 1.20. The covalent immobilization of *per*-azido- β -CD onto the SiO₂ substrate was proved by fluorescence intensity enhancement, due to the formation of triazole rings on the alkyne- β -CD surface. The patterns formed were also visualized by fluorescence microscopy before and after incubation of alkyne- β -CD surfaces in a solution of a sulforhodamine B acid chloride-labelled divalent adamantyl guest (rhodamine Ad₂). The guest molecules were only observed where β -CD molecules were immobilized. This also confirmed the presence and correct orientation of the β -CDs on the surface.

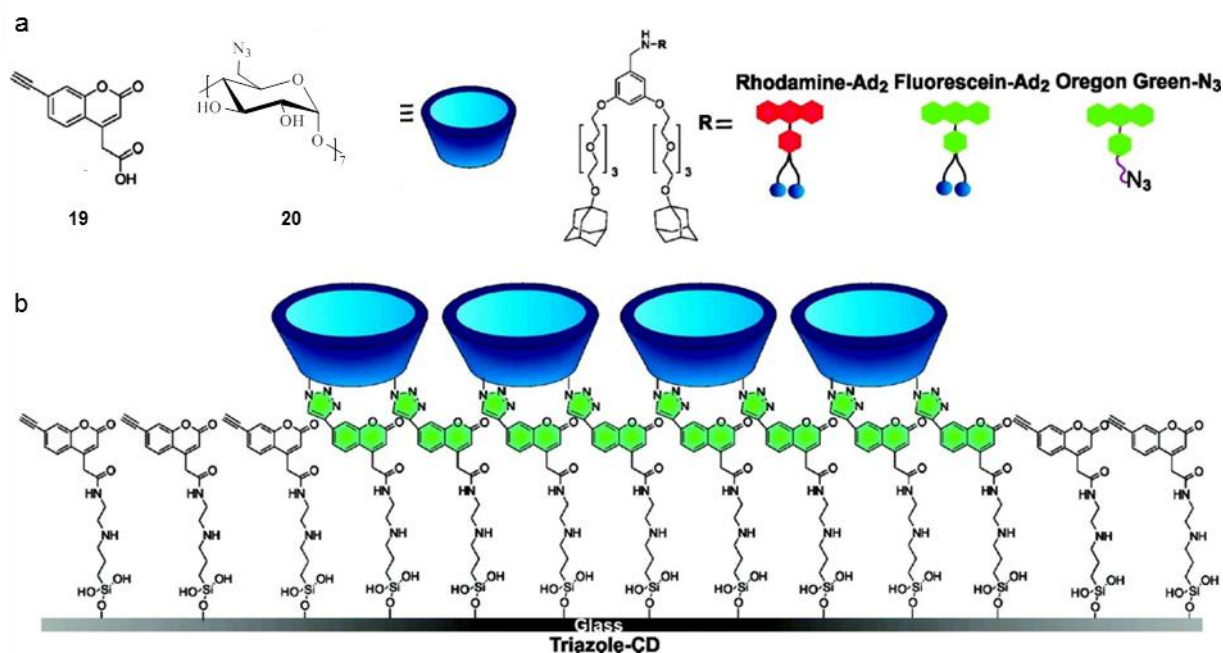


Figure 1.20 : a) Chemical structure of coumarin, *per*-azido- β -CDs, labelled diadamantyl guest and azide-functionalized dye; b) schematic representation of the patterned alkyne- β -CD monolayer prepared by μ CP of *per*-azido- β -CDs onto coumarin terminated monolayers (Reproduced with permission from Ref.78. © American Chemical Society, 2010.)

β -CD molecular printboards (using gold as a substrate) were also used as platforms for “writing” with supramolecular host molecules using a dip-pen nanolithography approach.⁶⁹ To that end, an AFM tip was used to transfer adamantyl-functionalized guests onto the printboard; a resolution below 100 nm was achieved with this approach. Maury *et al.* described a process for patterning CD monolayers on SiO₂ surfaces via nano-imprint lithography and consequently used it as a platform for fabrication of 3D nanostructures.¹⁰ First, β -CD patterned monolayers were formed on a silicon oxide surface through the attachment of the *per*-6-amino- β -CD (NH-CD) on an isothiocyanate-terminated monolayer. Those patterned SAMs were then used as starting points to build three-dimensional objects through a layer-by-layer approach using two types of nanoparticles (Au 2.8 nm, SiO₂ 60 nm), as shown in Figure 1.21.

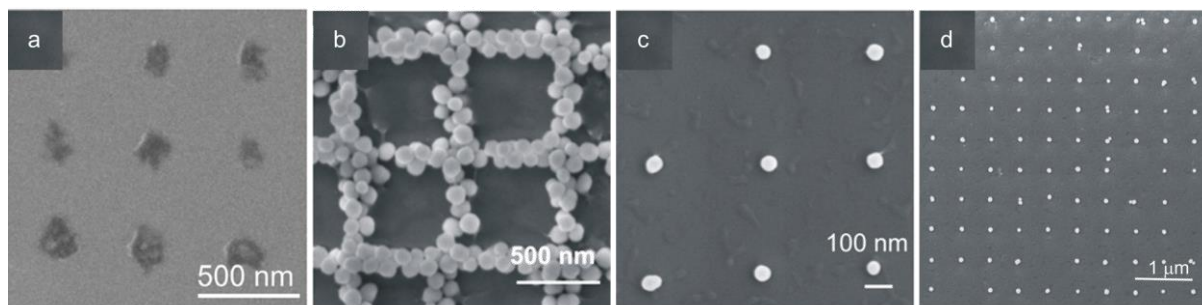


Figure 1.21: SEM micrographs of nano-imprint lithography-patterned CD-layers followed by supramolecular host-guest assemblies of a) fifteen bilayers of adamantyl-functionalized dendrimers and CD functionalized Au NPs with 200 nm dot features; b) two bilayers (with 150 nm wide grids); c) one bilayer of the adamantyl functionalized dendrimers and CD functionalized SiO₂ NPs with 60 nm dots pattern forms; d) single NPs (60 nm) on a periodic pattern (Reproduced with permission from Ref.10. © IOP Science, 2007.)

Harada *et al.* used CD polymer based gel systems to demonstrate molecular recognition at the macroscopic scale.⁷⁹ A polyacrylamide-based hydrogels possessing either CDs as hosts or organic guest moieties (*i.e.*, adamantyl, *n*-butyl or *t*-butyl) known to form complexes with CDs were synthesized. These gels were produced as millimetre-size cubes and doped with dyes to allow for visual differentiation. They demonstrated that a strong affinity exists between β -CD gel and adamantyl-gel in water, owing to the complexation of the host and guest molecules (Figure 1.22). The study of Harada certainly represents one of the first studies showing that recognition phenomena taking place at the molecular level can impact the assembly of millimetre-size objects.

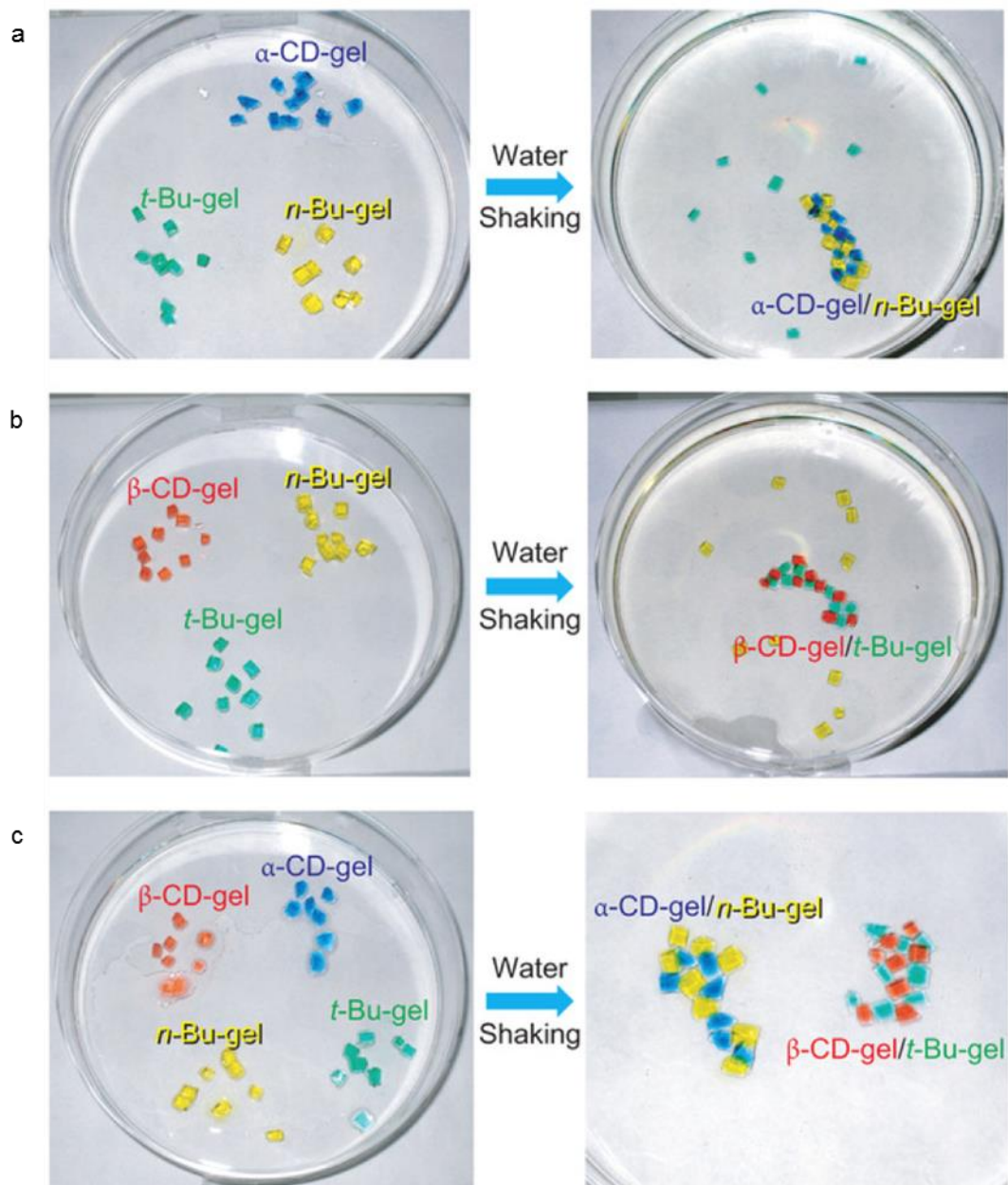


Figure 1.22: Specific molecular recognition visualized at macroscopic scale (Reproduced with permission from Ref.79. © Nature, 2011.)

Chapter 2. Results and discussion

2.1. Reversible supramolecular modification of membrane surfaces

Enzymes are used as catalysts for a wide range of chemical reactions with good substrate selectivity, regio- and stereo-selectivity.⁸⁰⁻⁸³ Therefore, they have an important role for the development of industrial biotechnology processes. In order to use enzymes in continuous reactor systems, they need to be retained either by using ultra- or nano-filtration membranes or by chemical immobilization on solid substrates.⁸⁴⁻⁸⁷ However, ultra- or nano-filtration requires large amounts of energy in order to reach a reasonable flow rate and is often limited by fouling issues. The second approach is also limited by the limited stability of the enzyme under operational conditions.

In order to overcome these limitations, we developed a surface modification strategy that allows for the reversible immobilization of active enzyme-polymer conjugates at the surface of polyethersulfone (PES) filtration membranes. We used this approach to design a membrane bioreactor in which a β -galactosidase (β -gal) enzyme is immobilized in a stable yet reversible fashion.⁸⁸ This strategy is based on multiple host-guest supramolecular interactions between enzyme-polymer conjugates and membrane surfaces. We used a multivalent water-soluble guest and a host molecule (β -cyclodextrin, β -CD) covalently attached at the surface of PES membranes. In order to introduce reactive functional groups at the membrane surfaces, we followed an UV photo-grafting strategy. One of the advantages of this method is the possibility to be applied in large scales for industrial applications. The PES membranes were chemically modified using a coupling reaction between activated carboxylic acids and primary amine functions. This was achieved by introducing carboxylic functions on PES surfaces and synthesizing an amino derivative of β -CD (NH-CD).

2.1.1. Covalent modification of PES membranes

2.1.1.1. PES membranes

Different polymeric materials can be used for organic membrane production such as poly(vinyl alcohol), polyamide, poly(acrylic acid), PES, polypropylene and poly(methyl methacrylate), to name but a few.⁸⁹ PES membranes are one of the most used materials for the formulation of organic membranes (Figure 2.1). This widespread use is due to their low cost and good process-ability, chemical, thermal and mechanical resistance. PES membranes find applications in different fields such as chemical industries, protein purification and water treatment.⁹⁰

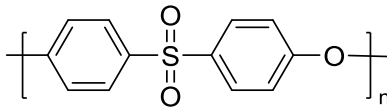


Figure 2.1: Chemical structure of polyethersulfone (PES)

One of the disadvantages of PES membranes is their hydrophobic character, which prevents spontaneous wetting with aqueous media.⁹¹ Different procedures were proposed to render the surface of the membranes more hydrophilic. For instance, membranes can be prepared from a mixture of sulfonated and non-sulfonated polysulfone.^{92,93} The sulfonation can be controlled in order to limit the water solubility of the polymer. Another disadvantage of PES membranes possessing (nano)-structures on the surface is their high level of fouling, which can cause fast deterioration of membrane permeability.^{92,94} It was demonstrated that the fouling resistivity of PES membranes could be significantly increased by applying photo-graft copolymerization of neutral hydrophilic monomers.⁹⁵ Indeed, photo-grafting methods compared with other methods such as plasma activation offers some advantages such as mild reaction conditions and low cost.

Polymeric filtration membranes are also used as support materials for the immobilization of different catalysts such as enzymes.⁹⁶⁻⁹⁸ Hilal *et al.* demonstrated that lipases can be immobilized on PES ultrafiltration membranes.⁹⁸ The membranes with immobilized enzymes on their surfaces offer the advantage to operate simultaneously as a catalytic support and selective barrier.^{99,100} Nevertheless this method is limited by the low temporal stability of the enzymes. Indeed when the bio-catalytic activity of enzymes deteriorates, the membrane has to be replaced.

2.1.1.2. Introduction of carboxylic functions on PES membrane surfaces (AA-PES)

A UV photo-grafting approach was developed for introducing carboxylic acid functions at the surface of the membrane. UV irradiation results in the partial homolysis of the PES polymeric chain, essentially at the surface of the material.¹⁰¹ The radicals formed can then react with alkenes via a homolytic addition mechanism. In this work, this was achieved by incubating the membrane material in an aqueous solution of acrylic acid followed by UV irradiation. This led to the covalent grafting of the acrylic acid monomer and to the introduction of carboxylic acid functions at the surface of the membrane (AA-PES). The membranes were analysed by means of Fourier-transform infrared spectroscopy (FTIR). The appearance of the carboxylate carbonyl stretching vibration band at 1708 cm^{-1} , corresponding to carboxylic acid functions, confirmed the effective immobilization of acrylic acid on the membrane surface (Figure 2.2).

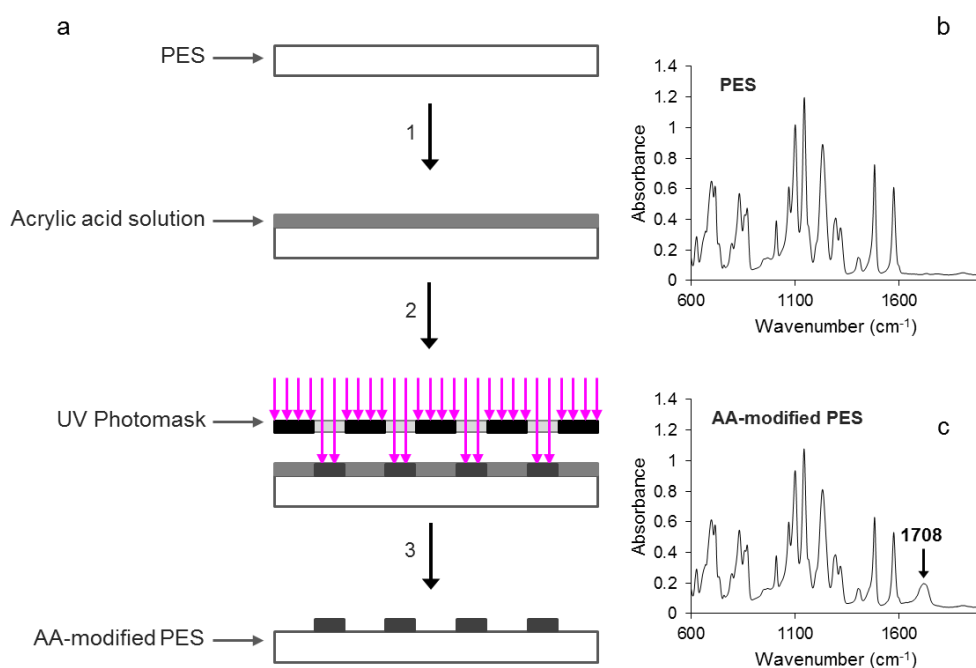


Figure 2.2: (a) Schematic representation of the synthetic route to introduce carboxylic functions at the surface of PES membranes in a micro-patterned fashion; FTIR absorbance spectra characterization of (b) bare PES membrane and (c) PES membranes modified with acrylic acid.

In order to introduce sufficient carboxylic acid functions at the surface of the membranes and to avoid membrane fouling, the carboxylic acid immobilization was optimized. Optimizations were achieved by varying UV irradiation time (0-330 sec) and monitoring the water flow through the membrane and relative intensity of carbonyl band at the surface of the membranes using FTIR; *cf.* Figure 2.3.

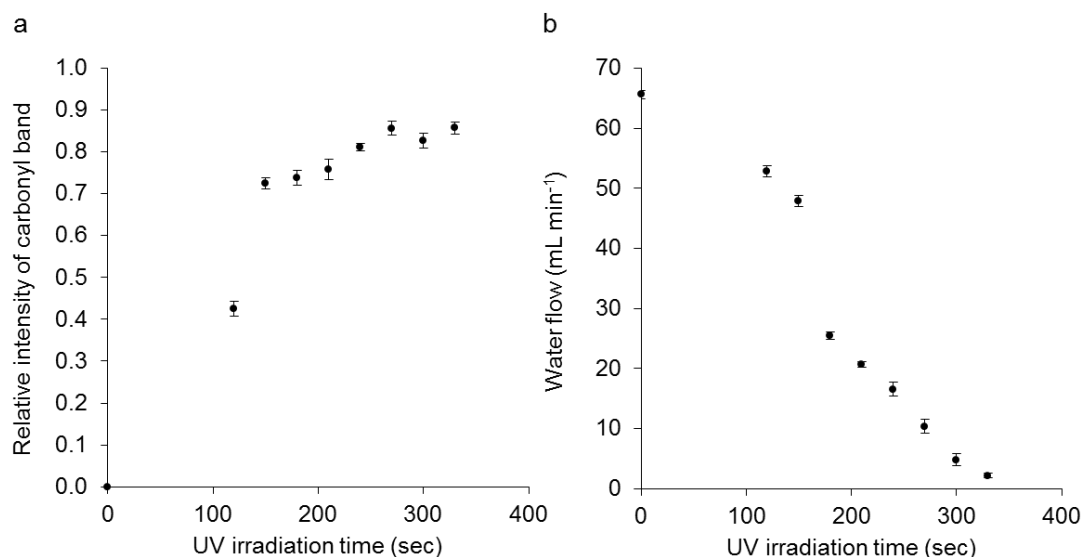


Figure 2.3: Assessment of carboxylic acid immobilization at the surface of the AA-PES membranes; (a) measurements of relative intensities of carbonyl bands of AA-PES membranes as a function of UV irradiation time; (b) measurements of water flow through AA-PES membranes as a function of UV irradiation time.

By increasing the UV irradiation time from 0 to 330 sec, the relative intensity of the carbonyl band increased from 0 to 0.86, while the water flow through the AA-PES membrane decreased from 65 to 2 mL min⁻¹. After 150 seconds of UV irradiation time, the water flow through the membrane decreased only of 15% while the relative intensity of the carbonyl band at the surface of PES was 84% of the maximum intensity measured. Therefore we used 150 sec UV irradiation time as the optimized condition for introducing carboxylic acid functions at the surface of the membranes.

In addition to membranes fully exposed to UV irradiation, membranes photo-patterned were produced using a UV photomask (100 × 100 μm squares). These membranes were used for the microscopic assessment of the supramolecular host-guest binding as the non-UV-exposed surface represented an internal reference.

The membranes fully exposed to UV irradiation were further characterized with Field-emission scanning electron microscopy (FE-SEM) and atomic force microscopy (AFM). No significant differences in morphology of the membranes were observed before and after treatment (Figure 2.4). The results revealed that the surface roughness measured by AFM before (202 nm) and after modification (191 nm) did not change significantly.

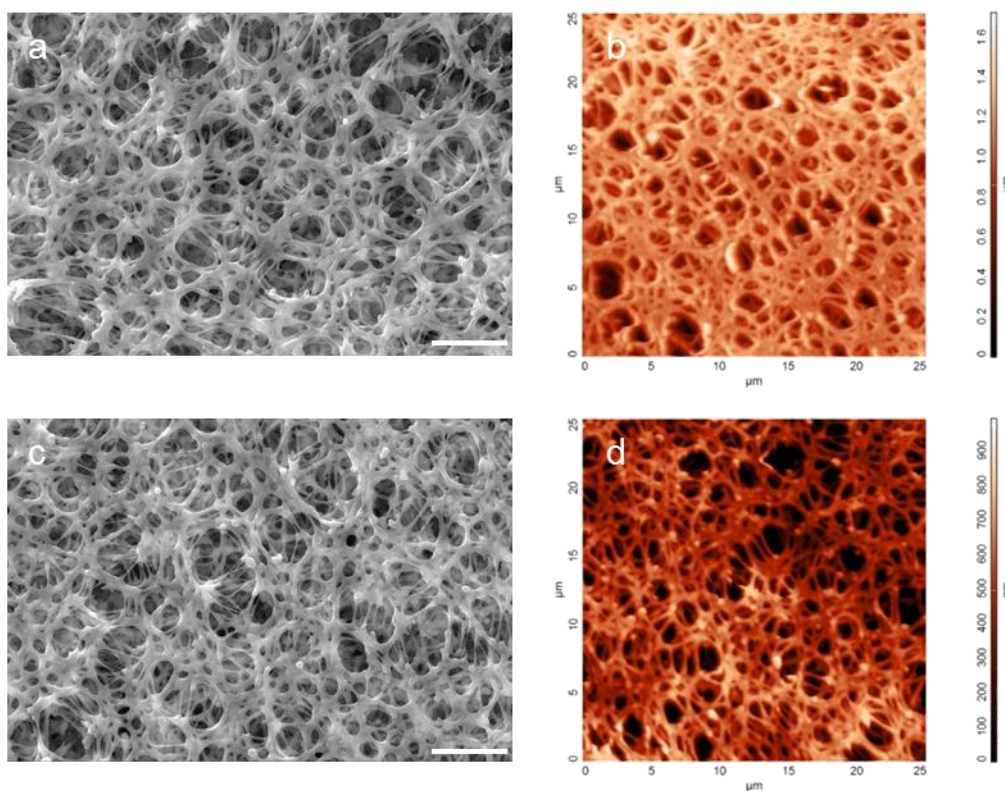


Figure 2.4: FE-SEM micrographs of (a) PES and (c) AA-PES. AFM tapping mode micrographs (25 μm scan range) of (b) PES and (d) AA-PES. Scale bars represent 5 μm .

2.1.1.3. Synthesis of heptakis(6-deoxy-6-amino)- β -cyclodextrin (NH-CD)

In order to immobilize CDs at the surface of AA-PES membranes, heptakis(6-deoxy-6-amino)- β -cyclodextrin (NH-CD) was synthesized from β -CD in three steps (Figure 2.5).¹⁰² First the *per*-6-iodo derivative of β -CD was prepared (yield 81%) from the native β -CD via an Appel conversion using triphenylphosphine and iodine. The reaction was followed by the nucleophilic substitution (S_N2) of the iodine by azido functions using sodium azide to yield the *per*-6-azido- β -CD derivative (yield 90%). The azide functions were consecutively reduced to the corresponding amine groups using triphenylphosphine and aqueous ammonia to yield the *per*-amino derivative of β -CD (yield 92%). The three molecules synthesized were characterized with nuclear magnetic resonance (^1H NMR, ^{13}C NMR) and matrix-assisted laser desorption/ionization time of flight mass spectroscopy (MALDI-TOF). The analytical data were in perfect agreement with those reported in the literature.¹⁰²

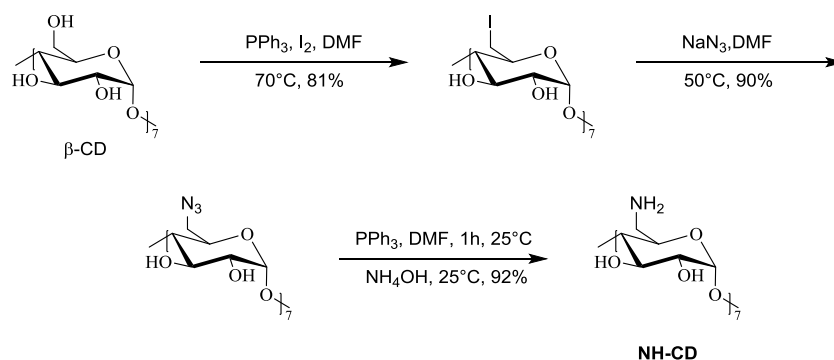


Figure 2.5: Synthetic route to NH-CD

2.1.1.4. Immobilization of NH-CDs on the AA-PES membranes

The NH-CDs synthesized were immobilized on the surface of AA-PES membranes following a procedure described hereafter. The carboxylic functions at the surface of the membranes were activated using 1-ethyl-3-(3-dimethylaminopropyl)carbodiimide (EDC) in order to yield active *O*-acylisourea intermediates. This reaction was followed by the nucleophilic attack of the primary amino groups of NH-CD to the activated leaving groups, which resulted to formation of the desired amide (NH-CD-PES) (Figure 2.6).

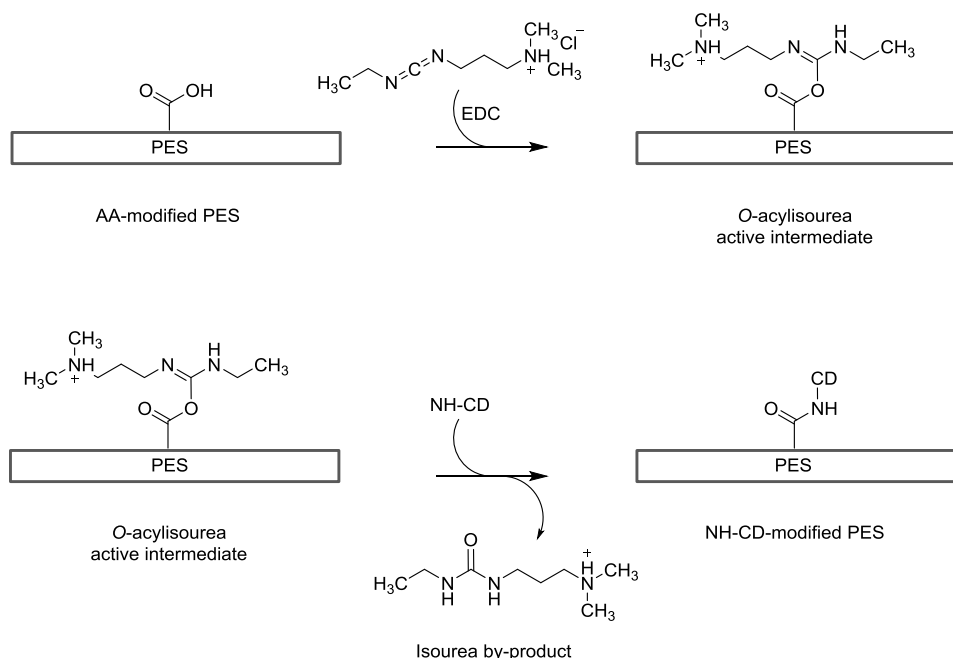


Figure 2.6: EDC reacts with carboxylic acids to create an *O*-acylisourea intermediate. In the presence of NH-CD, an amide bond is formed with release of an isourea by-product.

The CD-modified membranes were characterized with FTIR. The FTIR absorbance spectrum of NH-CD-PES membrane was compared with AA-PES membrane. The successful NH-CD

coupling was confirmed by a decrease in intensity of the carbonyl stretching band measured at 1708 cm^{-1} for the carboxylic acid and the appearance of the stretching band of the amide carbonyl (which resulted from the coupling to the amine functions of NH-CD) at 1641 cm^{-1} ; *cf.* (Figure 2.7). The topography of the membrane surface was monitored after immobilization of NH-CD using FE-SEM. No significant change in morphology was observed compared to AA-PES membrane. Additionally, the surface roughness of 206 nm measured by AFM also confirmed no significant alternation.

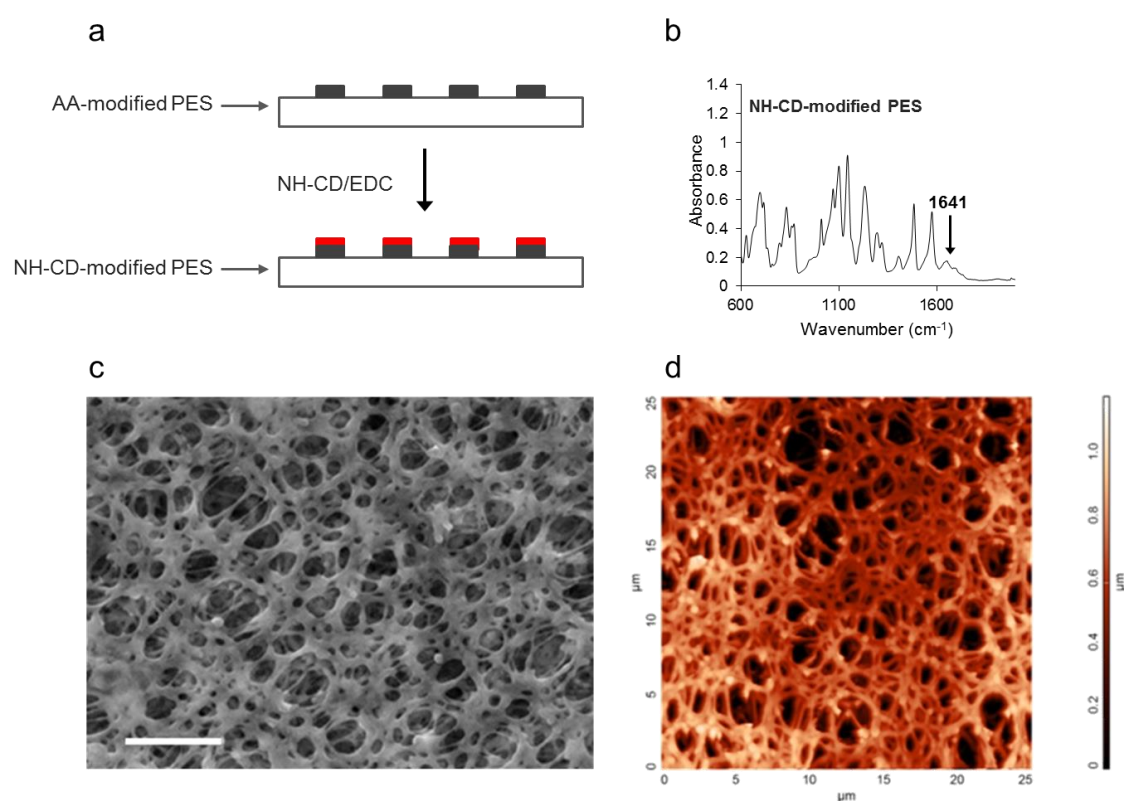


Figure 2.7: (a) Schematic representation of the synthetic route to introduce NH-CDs at the surface of AA-PES membranes in a micro-patterned fashion; (b) FTIR absorbance spectra of NH-CD-PES membrane; (c) FE-SEM micrographs of PES; (d) AFM tapping mode micrograph (25 μm scan range) of a NH-CD-PES. Scale bars represent 5 μm .

2.1.2. Synthesis of the multivalent enzyme-polymer conjugate (MEP)

The enzyme-polymer conjugate (MEP) to be used to bind to CD-modified membranes, besides the water solubility needed for the enzyme activity, has to possess multiple chemical functional groups able to form inclusion complexes with the CDs macrocycles immobilized on the surface of the membrane. We synthesized an acrylamide-based polymer using three different monomers, namely adamantyl acrylamide, acryloyl-6-aminocaproic acid and acrylamide as monomers. Adamantyl acrylamide was synthesized by the amidification of 1-

adamantylamine using acryloyl chloride and trimethylamine (Figure 2.8). All analytical values (^1H NMR, ^{13}C NMR) were in good agreement with those reported in the literature.⁷⁹

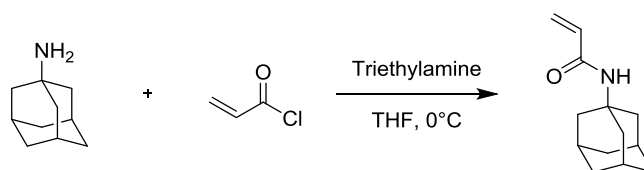


Figure 2.8: Synthetic route to adamantyl acrylamide

A soluble “guest polymer” was synthesized by the copolymerization of acrylamide, acryloyl-6-aminocaproic acid and adamantyl acrylamide via radical polymerization using azobisisobutyronitrile (AIBN) in dimethyl sulfoxide (Figure 2.9).⁷⁹ The polymer was purified by dialysis and characterized using NMR and gel-permeation chromatography (GPC). The preliminary results of GPC revealed that polymer synthesized had a very high polydispersity. Consequently the precise average molecular weight of the polymer and consequently the number of adamantyl functions per polymer could not yet be extracted from the characterization results. Therefore, we optimized the reaction conditions and used a reversible addition-fragmentation transfer (RAFT) method. RAFT polymerization is one of the most efficient methods for polymer synthesis with controlled molecular weight and low polydispersity.¹⁰³

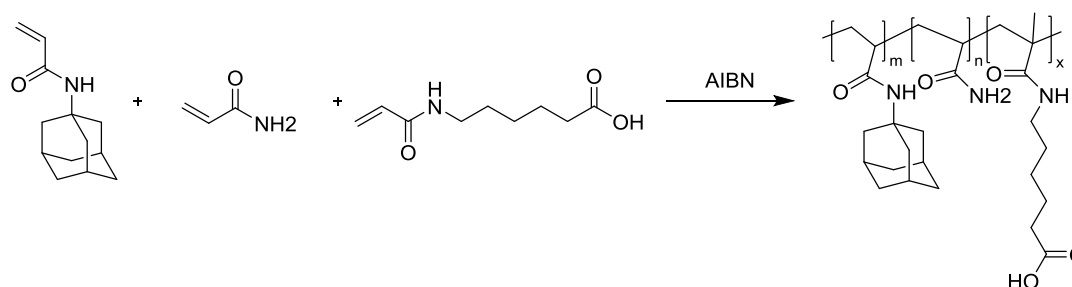


Figure 2.9: Synthetic route to a soluble guest polymer

Using the same monomer as acrylamide, acryloyl-6-aminocaproic acid and adamantyl acrylamide, the polymer was synthesized following a RAFT strategy (Figure 2.10).

The acrylamide-based polymer was characterized by GPC, which revealed a weight average molecular weight of 11600 and a polydispersity index of 2.2. The weight average molecular

weight of the polymer synthesized corresponds to 8.1 adamantyl functions per polymer molecule.

In order to bio-functionalize the surface of the filtration membranes, an enzyme namely β -galactosidase (β -gal; EC 3.2.1.23) from *Kluyveromyces lactis* had to be covalently attached to the polymer synthesized. The carboxylic functions of this polymer were activated using EDC and N-hydroxysulfosuccinimide (sulfo-NHS) and reacted with β -gal in a phosphate buffer. Subsequently, in order to follow in real time the supramolecular interactions between the water-soluble polymers synthesized and CDs immobilized on the membrane surfaces by fluorescent microscopy, the enzyme-polymer conjugate was labelled with a fluorescent dye (Fluorescein isothiocyanate, FITC); *cf.* Figure 2.10. We measured the enzymatic activity of MEP in solution. The results did not show any extreme loss in the activity of the enzyme after coupling with the polymer. As a control we also labelled β -gal with FITC.

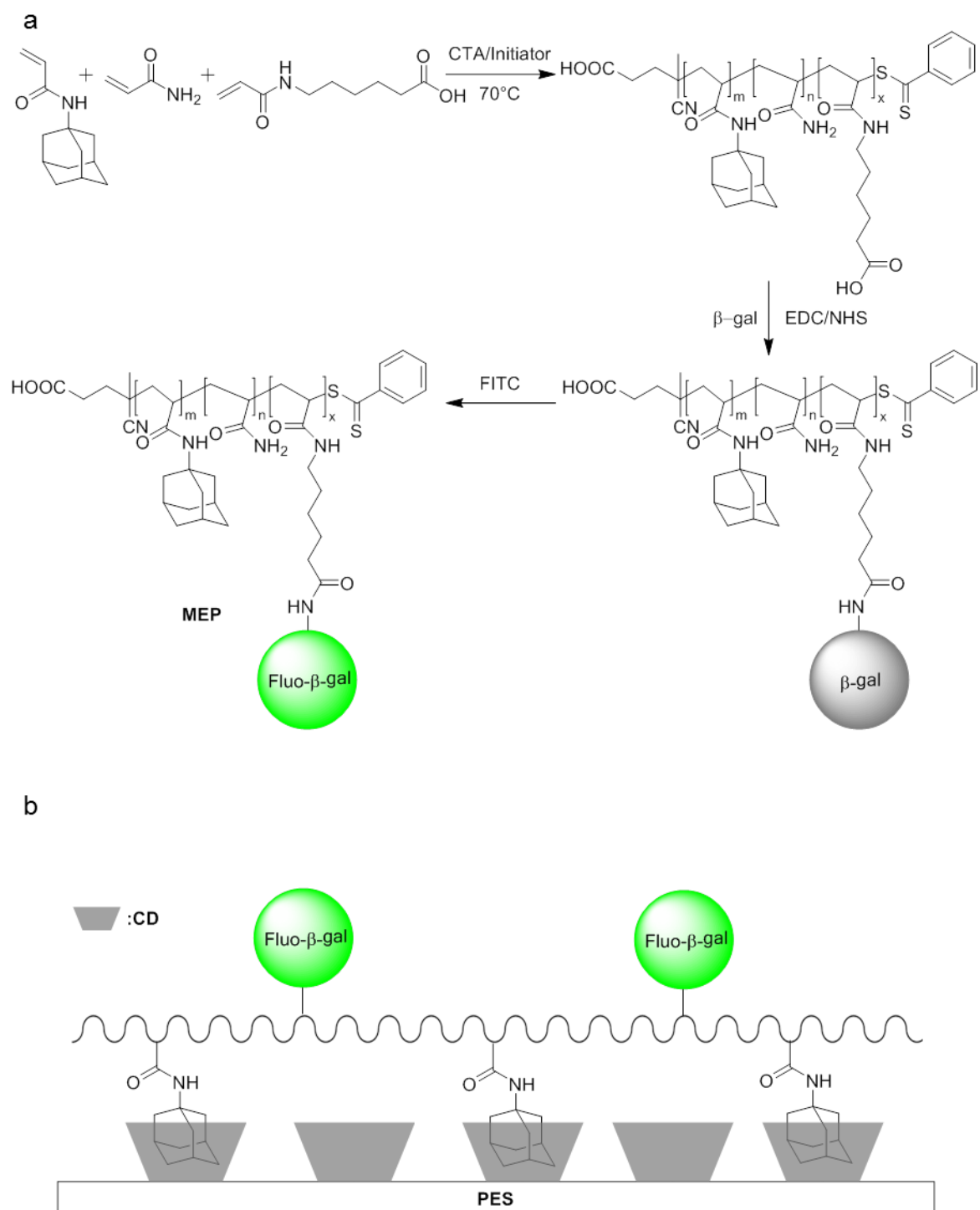


Figure 2.10: (a) Synthetic route to the fluorescently labelled MEP; an acrylamide-based polymer was synthesized following a RAFT strategy, using 4,4'-azobis(4-cyanopentanoic acid) as a radical initiator and 4-cyanopentanoic acid dithiobenzoate as a chain transfer agent. Adamantyl acrylamide, acrylamide and acryloyl-6-aminocaproic acid were used as monomers with molar ratio of 1:15:1. The synthesis was followed by covalent attachment of β -gal and subsequent labelling with a FITC; (b) Schematic representation of the multivalent supramolecular binding of MEP to covalently immobilized CDs on the membrane surface.

A water-soluble reference polymer (MEP_{ref}) was synthesized following the same protocol but excluding the guest moiety (adamantyl-acrylamide monomer) (Figure 2.11). The GPC analysis of MEP_{ref} revealed a molecular weight of 4500 and a polydispersity index of 1.7. The lower

molecular weight of MEP_{ref} compared to MEP can be explained by to the absence of adamantyl acrylamide in MEP_{ref} synthesis, this monomer may have a slightly different chemical reactivity than that of the two other monomers used in the synthesis.

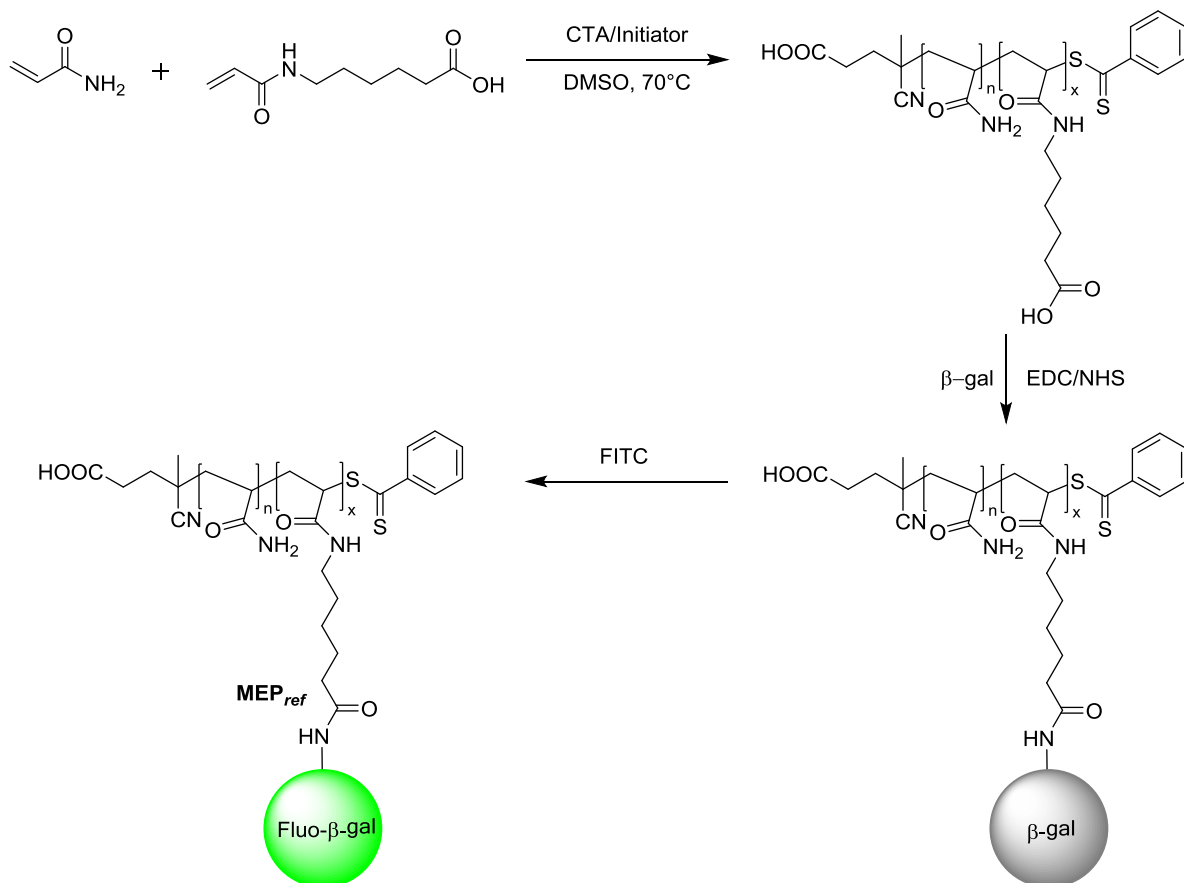


Figure 2.11: Synthetic route to fluorescently labelled MEP_{ref} ; an acrylamide-based polymer was synthesized following a RAFT strategy, using 4,4'-azobis(4-cyanopentanoic acid) as a radical initiator and 4-cyanopentanoic acid dithiobenzoate as a chain transfer agent. Acrylamide and acryloyl-6-aminocaproic acid were used as monomers with molar ratio of: 1:15. The synthesis was followed by covalent attachment of β -gal and subsequent labelling with a FITC.

2.1.3. Surface attachment of the multivalent enzyme-polymer conjugates

The supramolecular binding between multivalent enzyme-polymer conjugates (MEP) and immobilized NH-CDs on the surface of membranes was assessed using fluorescence microscopy and by monitoring a bio-catalytic conversion at the surface of the MEP-modified membranes.

2.1.3.1. Assessment of reversible surface modification by fluorescence microscopy

In order to study the supramolecular reversible binding of MEP and β -CD immobilized on the surface, the NH-CD-PES membranes were incubated in a solution of MEP for 30 min. In order to remove all molecules physisorbed, the membranes were thoroughly rinsed with nanopure

water and subsequently characterized by fluorescence microscopy. Five different control experiments were carried out by incubating NH-CD-PES membranes in solutions of Fluo- β -gal and MEP_{ref} and incubating PES, UV-irradiated PES membranes and AA-PES membranes in MEP solution. The results obtained are presented in Figure 2.12.

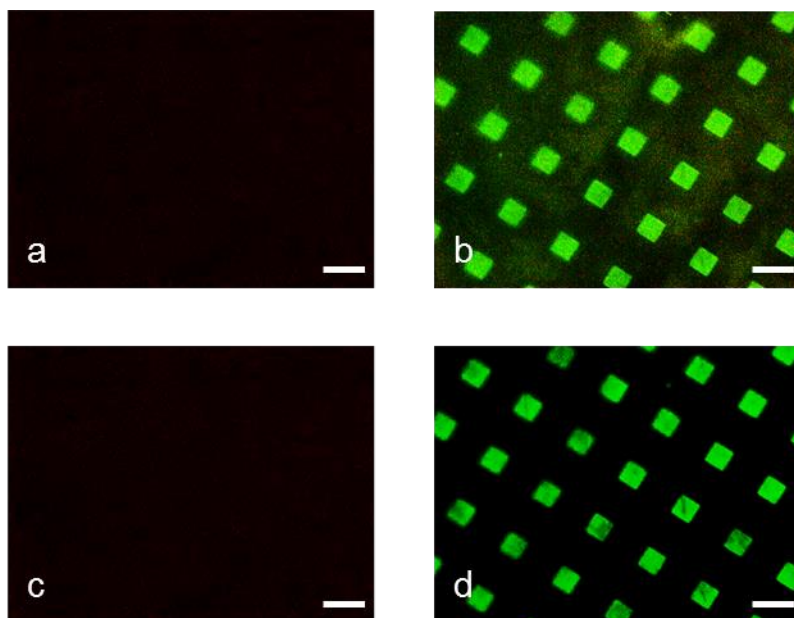


Figure 2.12: Fluorescence micrographs of the NH-CD-PES membrane, (a) before (NH-CD-PES) and (b) after incubation in MEP solution; (c) after incubation in a solution of β -CD and (d) after a second incubation in MEP solution. Scale bars represent 200 μ m.

After incubation with MEP, the NH-CD-PES membrane showed fluorescent square patterns with a size identical to that of the photomask we used for patterning the surface, thus confirming the attachment of the fluorescent MEP on CD-modified areas of the membrane. No other reference showed any relevant fluorescent signal, which proved the specific binding of MEP on CD-modified areas of the PES membrane. The reversibility of the supramolecular binding of MEP on NH-CD-PES surface was studied by rinsing the membranes with an aqueous solution of β -CD (20 g L⁻¹). As the supramolecular binding between MEP and β -CDs immobilized on the surface is expected to be under a dynamic equilibrium; the soluble β -CDs will compete with the ones immobilized. As a result, each adamantyl moiety of MEP will form a complex with soluble β -CD and it is anticipated that MEP will be released from the membrane surface. This hypothesis was confirmed, as no fluorescence signal was detected after washing the NH-CD-PES surface with β -CD solution. The reversibility of the process was confirmed by repeating the MEP incubation and recovering the original fluorescence pattern.

2.1.3.2. Bio-catalytic conversion at the surface of the MEP-modified membranes in a batch process

As a first experiment, we assessed the bio-catalytic conversion at the surface of the MEP-modified membranes in a batch process. A model reaction was used with *ortho*-nitrophenyl- β -galactoside (ONPG) as a synthetic substrate. In the presence of β -gal, ONPG is hydrolysed to galactose and *o*-nitrophenol. The CD-modified membranes were incubated in a MEP solution (0.01 g L^{-1}) for 30 min. Subsequently, in order to remove the unbound MEP, the membranes were thoroughly rinsed with buffer. In parallel, a series of control experiments were performed by incubating NH-CD-PES membranes with the enzyme (β -gal) in free solution and MEP_{ref} or by incubating PES membranes, UV-irradiated PES membranes and AA-PES membranes with a solution of MEP. The immobilized enzymatic activities on the PES membranes were measured using the conventional ONPG assay; the results are presented in Figure 2.13.

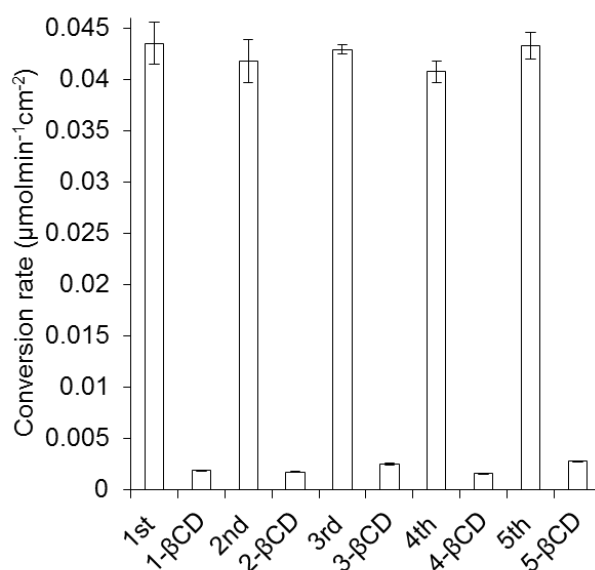


Figure 2.13: Measurements of ONPG conversion rates at the surface of membranes in a batch process after incubation of NH-CD-PES membranes in MEP solution, followed by incubation in a β -CD solution as a competitor host. The procedure was repeated five times.

For all control membranes, the ONPG conversion rates measured were lower than $0.002 \mu\text{mol min}^{-1} \text{cm}^{-2}$. However, a considerably higher ONPG conversion rate of $0.043 \mu\text{mol min}^{-1} \text{cm}^{-2}$ was measured for the MEP-modified membrane, which confirmed the selectivity of the adsorption of MEP on the surface. Additionally, the results obtained from this experiment proved that the catalytic characteristics of the enzyme were conserved after supramolecular immobilization of multivalent MEP at the surface of the PES membranes. After incubation of

the MEP-modified membranes in a β -CD solution, the ONPG conversion rate dropped to $0.0018 \mu\text{mol min}^{-1} \text{cm}^{-2}$ (Figure 2.13). This corresponds to a removal of 96% of the immobilized MEP from the PES surface. Subsequently, for a second cycle, MEPs were immobilized on the surface of the PES membranes. An activity of $0.042 \mu\text{mol min}^{-1} \text{cm}^{-2}$ corresponding to a recovery of 98% of the initial ONPG conversion rate was measured. After the second cycle of modification, the MEP-modified membrane could be regenerated, as the enzymatic activity dropped to $0.0017 \mu\text{mol min}^{-1} \text{cm}^{-2}$ after incubation in a β -CD solution. The MEP binding assay was repeated five times; after each cycle a recovery of 95-100% of the initial enzymatic activity was measured. The results obtained from this experiment confirmed the possibility to modify and regenerate the surface of PES membranes with MEP without significant loss of the enzymatic activity.

2.1.3.3. Bio-catalytic conversion at the surface of the MEP-modified membranes in a continuous filtration process

We also performed the supramolecular immobilization of MEP at the surface of PES membranes in a continuous filtration process. We fixed each filtration membrane using a disposable syringe filter holder while the flow rate of the fluid feed through the membranes was controlled using a syringe pump (Figure 2.14).

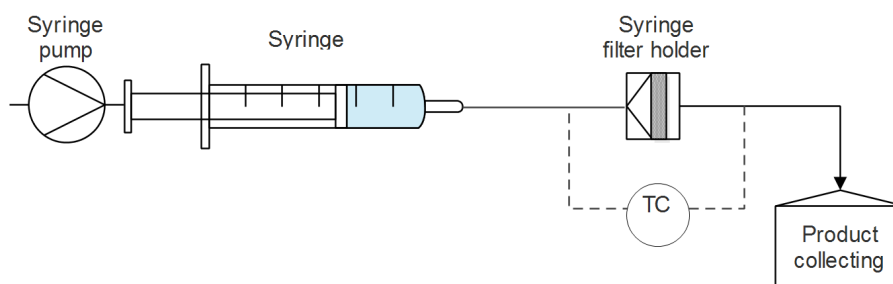


Figure 2.14: Schematic representation of the setup used for continuous filtration process

We first filtered the MEP solution (0.01 g L^{-1}) through the NH-CD-PES membranes with a flow rate of 4 mL h^{-1} . In order to evaluate the bio-catalytic conversion rate at the surface of the membranes, a solution of ONPG was subsequently filtered (4 mL h^{-1}) through the membranes at 40°C . The ONPG conversion rate at the surface of the MEP-modified membrane was measured to be $0.39 \mu\text{mol min}^{-1} \text{cm}^{-2}$, which is significantly higher than the value measured in the corresponding batch process ($0.043 \mu\text{mol min}^{-1} \text{cm}^{-2}$). Two hypotheses could explain the higher enzymatic activity at the surface of filtration

membranes in the continuous filtration process. The first hypothesis was that the substrate (ONPG) diffusion is a limiting factor in the batch process. The second hypothesis was that the density of immobilized MEP at the surface of NH-CD-PES membranes was higher when the immobilization was performed in a continuous filtration conditions.

In order to study substrate diffusion at the surface of PES filtration membranes in the batch process, we first incubated the MEP-modified membranes in solutions of ONPG at increasing concentrations going from 5 to 40 mM at 40°C. By increasing the ONPG concentrations, the bio-catalytic conversion rate at the surface of the MEP-modified membranes increased from 0.017 to 0.07 $\mu\text{mol min}^{-1} \text{cm}^{-2}$ until it reached a plateau (Figure 2.15).

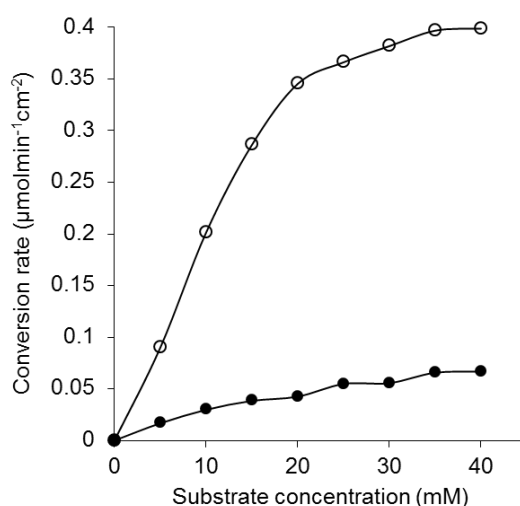


Figure 2.15: Measurements of ONPG conversion rates at the surface of the MEP-modified membranes in batch (●) and continuous (○) processes using increasing concentrations of ONPG.

These results confirmed that the ONPG diffusion is a limiting factor in the batch process. Nevertheless, the maximum enzymatic activity in the batch process ($0.07 \mu\text{mol min}^{-1} \text{cm}^{-2}$) was still lower than in the filtration process ($0.39 \mu\text{mol min}^{-1} \text{cm}^{-2}$). In order to better understand this difference, we modified the membranes with MEPs in a continuous filtration process and assessed their enzymatic activities in batches using different ONPG concentrations going from 5 to 40 mM. From the results shown in Figure 2.15, it could be seen that by increasing the substrate concentration, the enzymatic activity increased steadily from 0.09 to $0.39 \mu\text{mol min}^{-1} \text{cm}^{-2}$ until it reached a plateau. The maximum enzymatic activity in this experiment reached the value obtained in the filtration process. These results confirmed that both substrate diffusion and the quantity of immobilized MEP, are limiting the batch process. We confirmed that in the continuous filtration process, MEPs were also

immobilized within the membrane pores. Therefore the batch process compared to the continuous filtration process resulted in lower ONPG conversion rates.

2.1.3.4. Bio-catalytic conversion at the surface of the MEP-modified membranes in a continuous filtration process using a complex matrix

We assessed the efficiency and stability of the MEP-modified membranes under operational conditions in a complex matrix. To that end, we investigated the hydrolysis of lactose in milk serum. In such a complex matrix, the presence of high concentrations of small molecules that can compete with the adamantane-CD complex can decrease the stability of the immobilization and hinder the overall process. The assay was performed using the MEP-modified membranes. In parallel, as a control experiment, the soluble enzyme (β -gal) was filtered through the NH-CD-PES membrane. Consequently, milk serum was filtered through the MEP-modified and reference membrane at flow rate of 4 mL h^{-1} at 40°C . We measured then the immobilized enzymatic activities on the surface of the membranes (Figure 2.16)

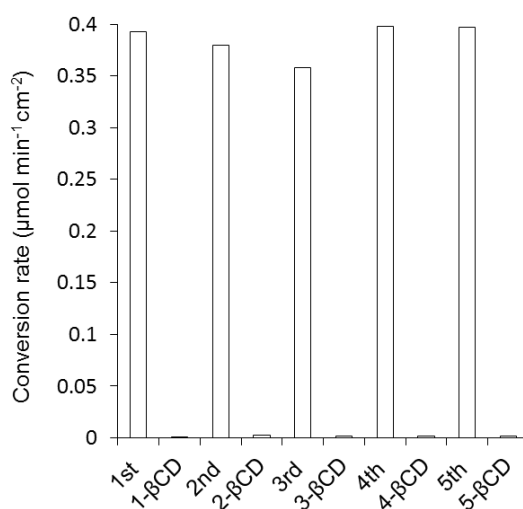


Figure 2.16: Measurements of lactose conversion rates at the surface of membranes after filtration of milk serum solution through the MEP-modified membranes, followed by filtration of a β -CD solution as a competitor host. The procedure was repeated five times.

The enzymatic activity at the surface of the reference membrane was only $0.003 \mu\text{mol min}^{-1} \text{cm}^{-2}$. The lactose conversion rate at the surface of the MEP-modified membrane was $0.39 \mu\text{mol min}^{-1} \text{cm}^{-2}$. The MEP-modified membranes have similar conversions rates for both substrates, namely lactose and ONPG. This is explained by the fact that β -gal has a similar maximum velocity for both substrates ($600 \mu\text{mol min}^{-1} \text{mg}^{-1}$).¹⁰⁴

In order to regenerate the MEP-modified membranes, a β -CD solution was filtered through the membranes with a flow rate of (4 mL h^{-1}). The enzymatic activity dropped to $0.0004 \text{ } \mu\text{mol min}^{-1} \text{ cm}^{-2}$, which confirmed that 99.9% of immobilized MEP was removed from the membrane surface. For a second cycle, the membranes were modified with MEP and a recovery of 98% ($0.38 \text{ } \mu\text{mol min}^{-1} \text{ cm}^{-2}$) of initial enzymatic activity was obtained. The MEP binding assay and assessment of the hydrolysis of lactose in milk serum was repeated for five times. After each cycle, we recovered 92-102% of the initial enzymatic activity. The results obtained from this experiment proved that the MEP-modified filtration membranes maintain their efficiency and stability in a complex matrix such as milk serum. Additionally it confirmed the possibility to regenerate the PES membrane without significant loss of enzymatic activity in milk serum.

2.1.4. Summary

In summary, we developed a new supramolecular strategy that allows immobilizing enzymes at the surface of filtration membranes in a stable and reversible fashion. Our approach is based on multiple point host-guest supramolecular inclusion interactions between CDs immobilized at the surface of the PES membranes and the enzyme-polymer conjugates. Low density of CDs as host entities were immobilized covalently at the surface of the polymeric filtration membrane. We synthesized an acrylamide-based polymer possessing adamantyl moieties as guest functions and β -gal as a biocatalyst. The bio-conjugation strategy is versatile as it is based on a coupling reaction between activated carboxylic acids of the polymer and primary amine functions of lysine of the enzyme and can therefore be applied to a wide range of enzymes. We demonstrated that this method allows the stable immobilization of an enzyme at the surface of filtration membranes. The membrane bioreactors developed allowed for an efficient hydrolysis of lactose in milk serum. This approach is expected to be important for different industrial bio-based applications.

2.2. Reversible supramolecular modification of surface resonance sensor (SPR) chip

Surface plasmon resonance (SPR) is an optical technique that is used to study molecular interactions on surfaces. It is a surface-sensitive bioanalytical method that allows for a rapid and label-free monitoring of bio-molecular interactions on the surface of a sensor in a real time.^{105,106} Binding of an analyte (*e.g.* antibody) from the solution to an immobilized bio-molecule (*e.g.* antigen) on a sensor chip results in a change of refractive index that is measured as a change in a wavelength.¹⁰⁶

In order to perform multiple analyses with a single sensor, the conjugate surface has to be regenerated by dissociation of antigen-antibody complex.¹⁰⁷⁻¹⁰⁹ However, once an antigen is inactive, the SPR sensor chip has to be replaced. It is therefore important to develop a more cost-effective method to regenerate the surface of a used SPR sensor chip for SPR-based immunoassays.

We adapted the strategy developed for membranes to stably but reversibly immobilize antigen-polymer conjugates at the surface of gold SPR sensor chips. This approach is based on multivalent interactions between an antigen-polymer conjugate and a SPR sensor chip surface. We used a multivalent acrylamide-based polymer guest and a host molecule (β -CD) covalently immobilized at the surface of gold SPR sensor chips (Figure 2.17). This approach allows to in-place regenerate the SPR sensor chips with new bio-molecules in SPR-based immunoassays.

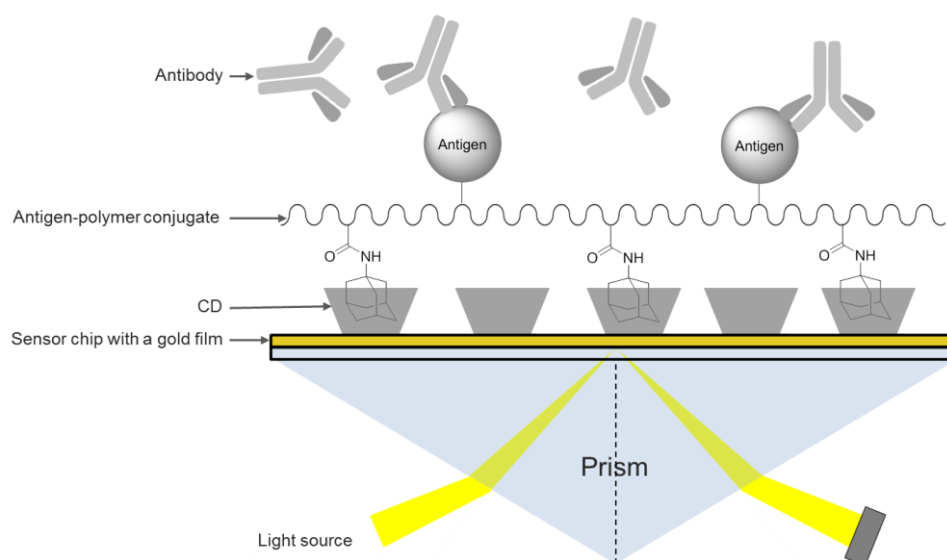


Figure 2.17: Schematic representation of a multivalent supramolecular binding of an antigen-polymer conjugate to covalently immobilized CDs on a SPR sensor chip surface.

2.2.1. Chemical modification of gold sensor chips

The chemical modification of gold sensor chips was based on the formation of highly ordered monolayers of a dialkylsulfide derivative of β -CD on a surface of a gold SPR sensor chip.

2.2.1.1. Synthesis of heptakis{6-deoxy-6-[12(thiododecyl)undecanamido]}- β -CD

In order to immobilize CDs at the surface of gold sensor chip, we synthesized heptakis{6-deoxy-6-[12(thiododecyl)undecanamido]}- β -CD. This was achieved following the synthetic route presented in Figure 2.18.

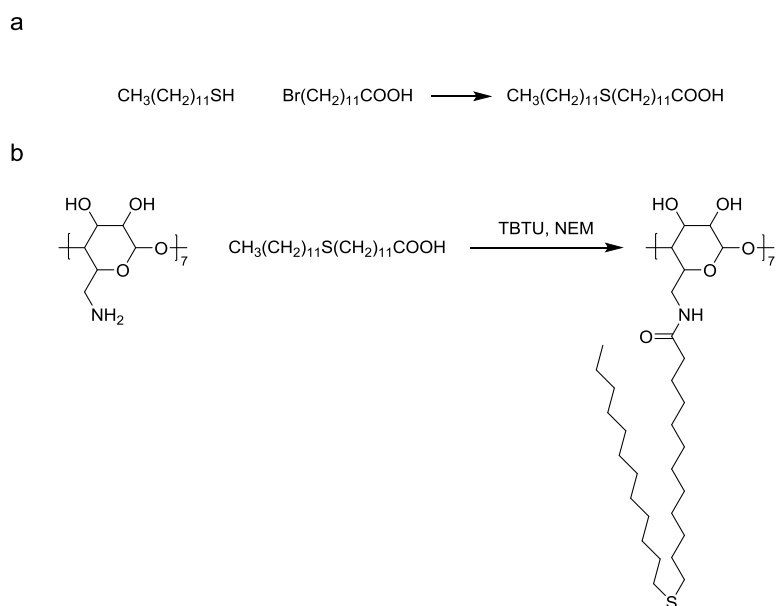


Figure 2.18: (a) Synthetic route to 12-(thiododecyl)undecanoic acid; (b) synthetic route to heptakis{6-deoxy-6-[12(thiododecyl)undecanamido]}- β -CD; *O*-Benzotriazol-1-yl-*N,N,N',N'*-tetramethyluronium tetrafluoroborate (TBTU) was used as an activating agent

12-(thiododecyl)undecanoic acid was synthesized by displacement of bromide from alkyl bromides by a thiolate anion (Figure 2.18). The resulting dialkyl sulphide was purified by crystallization in heptane. All analytical values (^1H NMR and ^{13}C NMR) were in good agreement with those published in the literature.¹¹⁰

A dialkyl sulfide derivative of β -CD was synthesized by reacting *per*-amino derivative of β -CD (NH-CD) and 12-(thiododecyl)undecanoic acid in presence of *O*-Benzotriazol-1-yl-*N,N,N',N'*-tetramethyluronium tetrafluoroborate (TBTU) as an activating agent in freshly dried dichloromethane. All analytical values (^1H NMR, ^{13}C NMR) were in good agreement with those reported in the literature.¹¹¹

2.2.1.2. Self-assembled monolayers of heptakis{6-deoxy-6[12(thiododecyl)undecanamido]}- β -CD on a gold substrate

A SAM of dialkylsulfide derivative of β -CD were prepared (Figure 2.19) by immersing freshly cleaned gold substrates in a solution of heptakis{6-deoxy-6-[12(thiododecyl)undecanamido]}- β -CD (1 mM, EtOH:CHCl₃, 1:2, v/v) for 16 h at room temperature. Subsequently the CD-modified Au substrates (CD-Au) were rinsed with chloroform and assembled in the SPR chip holder. Surface ellipsometric analyses revealed a β -CD layer thickness of 22 Å, which is consistent with a vertically oriented heptakis{6-deoxy-

6-[12(thiododecyl)undecanamido]}- β -CD molecular structure to the Au plane as represented in Figure 2.19.

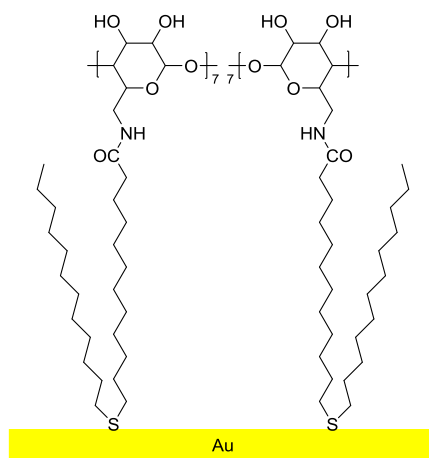


Figure 2.19: Schematic representation of a SAM of dialkylsulfide derivative of β -CD on a gold surface

2.2.2. Synthesis of the multivalent BSA-polymer conjugate (MPP)

In order to synthesize a multivalent antigen-polymer conjugate (MPP), we used the acrylamide-based polymer possessing adamantyl moieties as guest functions (section 2.1.2), which are able to form "host-guest" inclusion complexes with CDs immobilized on the surface of the CD-Au sensor chips. MPP was synthesized following the same protocol described for MEP (Figure 2.20), but using a protein that will serve as an antigen (bovine serum albumin, BSA) instead of an enzyme (β -gal).

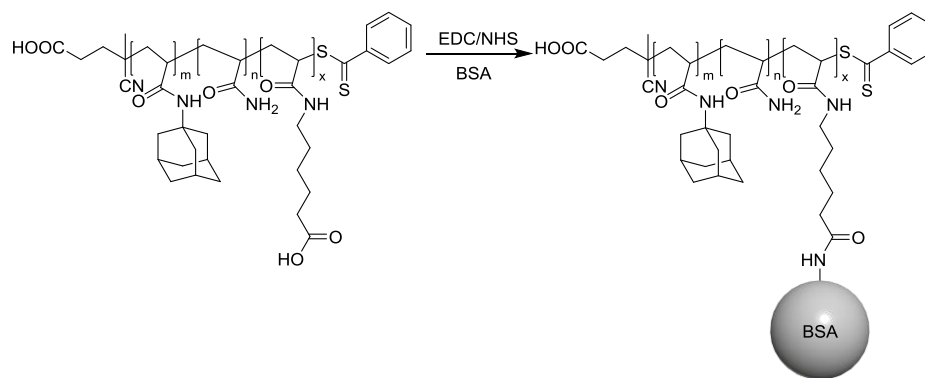


Figure 2.20: Synthetic route to MPP.

2.2.3. Assessment of the supramolecular binding of MPP on the chemically-modified SPR chips

NH-CD-Au sensor chips were equilibrated using HBS buffer (HEPES 0.01 M, NaCl 0.15 M, EDTA 3 mM, pH 7.4). After the equilibration stage, MPP (50 $\mu\text{g mL}^{-1}$) in HBS buffer was injected (5 $\mu\text{L min}^{-1}$) to one of the flow chambers. After injection of MPP and equilibration time of 15 min, the sensor response showed an increase of 511 arbitrary units (AU) (Figure 2.21). This proved the immobilization of MPP on the surface of the CD-Au sensor chip (MPP-Au).

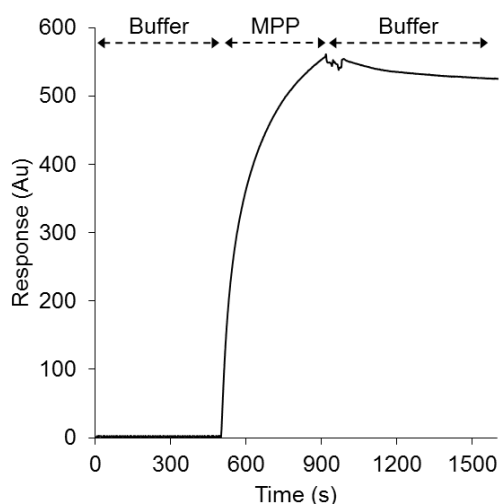


Figure 2.21: Binding sensogram of MPP, values are expressed in arbitrary units and normalized to zero at the beginning of the injection

In order to study the specific antigen-antibodies interactions between BSA and bovine serum albumin antibody (AntiBSA, 50 $\mu\text{g mL}^{-1}$), AntiBSA in HBS buffer was injected into both flow chambers (5 $\mu\text{L min}^{-1}$). A CD-modified flow chamber (CD-Au) was used as a reference flow chamber. After an equilibration time of 5 min, the sensor response was 102 AU higher in

MPP-Au than in the reference flow chamber (Figure 2.22), which proved the specific binding between AntiBSA and immobilized MPP on the surface.

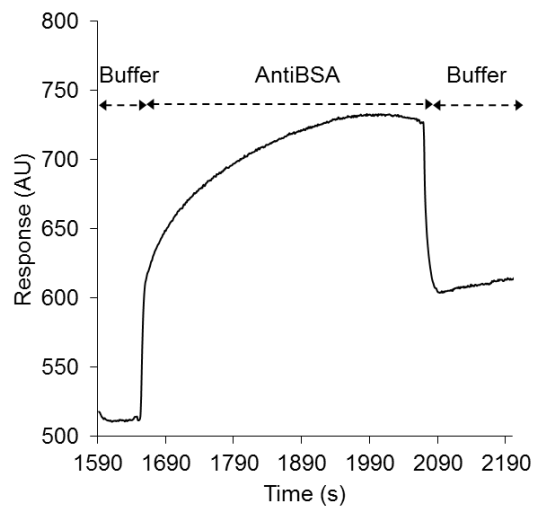


Figure 2.22: Binding sensogram of specific AntiBSA-MPP interactions

In order to dissociate the AntiBSA-BSA complex at the surface of the Au sensor chip, we injected glycine (10 mM, pH 2, 5 $\mu\text{L min}^{-1}$) to the AntiBSA-modified flow chamber. Most proteins become partly unfolded and positively charged at low pH. A decrease of 153 AU was measured after injection of glycine as a regeneration solution. This decrease in the signal response was close to the signal increase measured for immobilization of AntiBSA (102 AU) and thus proved AntiBSA removal (Figure 2.23).

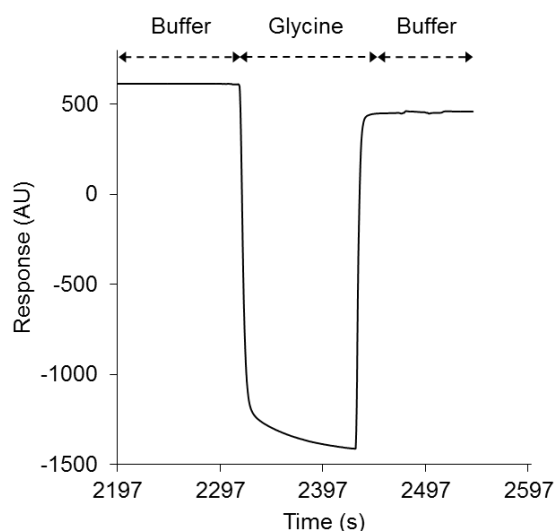


Figure 2.23: AntiBSA dissociation sensogram after loading of glycine solution

Furthermore, in order to regenerate the surface of MPP-Au sensor chips and remove MPP, we injected a solution of β -CD (20 g L^{-1}) as a competitor host. After four cycles of injection, a decrease of 430 AU was measured. This decrease in the signal response (430 AU) was close to the signal increase measured for immobilization of MPP (511 AU) and therefore proved MPP removal from the surface of the Au sensor chip (Figure 2.24).

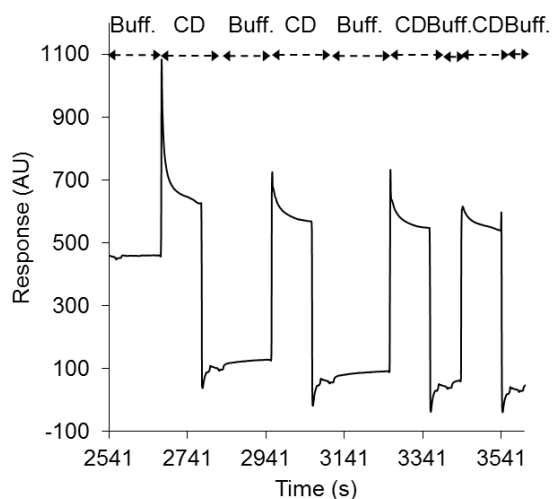


Figure 2.24: AntiBSA dissociation sensogram after injection of β -CD solution

The MPP binding assay and assessment of the AntiBSA-MPP was repeated another time. After the first cycle, 97% of the initial AntiBSA-MPP binding affinity was recovered (Figure 2.25). The results obtained from this experiment confirmed the possibility to modify and

regenerate the surface of Au SPR sensor chips with MPP without significant loss of antigen-antibody affinity.

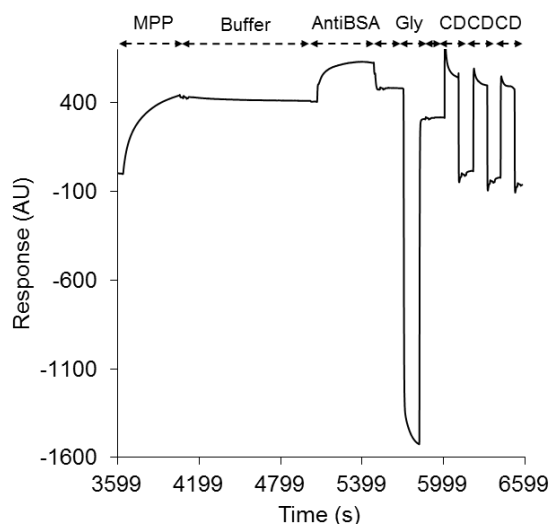


Figure 2.25: Binding sensogram of the regenerated Au sensor chip

2.2.4. Summary

We applied a similar supramolecular strategy used for reversible modification of filtration membranes, for reversible modification of Au SPR sensor chips. A SAM of the dialkylsulfide derivative of β -CD was prepared on a surface of Au sensor chips. An acrylamide-based polymer (MPP), possessing adamantyl moieties as guest functions and BSA as a ligand was synthesized following the same synthetic route used for MEP. This approach allowed for the stable but yet reversible immobilization of BSA at the surface of an Au SPR sensor chip. The MPP-modified SPR sensor chip allowed the assessment of an efficient antigen-antibody interaction. This approach can be theoretically used to immobilize a large variety of ligands on surface of SPR sensor chips and will allow using the same SPR sensor chip for several different immunoassays.

Chapter 3. Experimental methods

3.1. General

All solvents (analytical grade) were obtained from Sigma-Aldrich and used without further purification unless otherwise stated. Polyethersulfone filtration membranes were purchased from Millipore. A UV photomask (chrome/quartz) was obtained from Compugraphics Jena with 100×100 μm square features. Absorbance and fluorescence intensities were measured using a Biotek Synergy™ H1 Hybrid Multi-Mode Microplate Reader. All SPR binding assays were performed using a BIAcore® X apparatus. The gold SPR sensor chips (SIA Kit Au®) were obtained from BIAcore. Fluorescence microscopy images were acquired using an Olympus BX51 fluorescence microscope. Fourier transform infrared spectra were measured in attenuated total reflection (ATR) using a single reflection diamond ATR device (Golden Gate) and a Varian 670-IR spectrometer. Gel permeation chromatography (GPC) analysis was performed using an Agilent PL-GPC 50 Plus system. The instrument was equipped with refractive index (RI) detector. The following conditions were used for performing the GPC measurements: column, guard column and two PL-aquagel-OH Mixed-M columns; eluent, NaNO₃ (0.1 M) containing 10% MeOH (wt %) in water; flow rate, 1 mL min⁻¹; column oven temperature, 40°C. Polyethylene glycol standards were used for molecular weight calibration.

3.2. Synthesis of the enzyme-polymer conjugate (MEP)

All glassware was dried prior to use and DMSO was degassed with N₂ for 30 min. Subsequently, acrylamide (10.95 g, 154 mmol), adamantyl acrylamide (2.15 g, 10.5 mmol) and acryloyl-6-aminocaproic acid (1.94 g, 10.5 mmol) were dissolved in degassed DMSO (20 mL). 0.1 mmol of the radical initiator (4,4'-azobis(4-cyanopentanoic acid, 28 mg) and a 0.5 mmol of the chain transfer agent (4-cyanopentanoic acid dithiobenzoate, 139.7 mg) were added to the reaction mixture. The solution was purged with nitrogen for 30 min. The mixture was heated to 70° C for 24 h. The reaction mixture was cooled to the room

temperature and the product was precipitated in acetone three times. In order to purify the polymer, a dialysis (MWCO 3.5 kDa) was performed in water. The purified polymer was dried by lyophilisation.

An enzyme-polymer conjugate was synthesized by dissolving the polymer synthesized (1 g L^{-1}) in MES buffer (5 mM, pH 6). Subsequently, the activating agents, 1-ethyl-3-(3-dimethylaminopropyl)carbodiimide (2 mM) and N-hydroxysulfosuccinimide (5 mM) were added to the reaction mixture and the solution was stirred for 15 min at room temperature. The polymer was purified from reaction by-products by performing a dialysis (MWCO 3.5 kDa) in MES buffer. Consequently, β -gal (1:1, β -gal:polymer, molar ratio) was added to the activated polymer in sodium phosphate buffer (0.1 M, pH 7.5) for conjugation and the mixture was stirred for 2 h at room temperature. The enzyme-polymer conjugate was purified by performing dialysis (MWCO 50 kDa) in the enzyme buffer solution (dipotassium phosphate 100 mM, MgCl_2 5 mM, pH 6.5).

In order to label the enzyme-polymer conjugate, fluorescein isothiocyanate (FITC) was used. The enzyme-polymer conjugate buffer was exchanged to borate buffer (50 mM, pH 8.5) by dialysis (MWCO 10 kDa). After FITC was equilibrated at room temperature, it was dissolved in DMF (1 g L^{-1}) and was added to the enzyme-polymer conjugate solution (enzyme:FITC, 1:24, molar ratio). The solution was incubated at room temperature for 1 h. The excess of unreacted FITC was removed by doing a dialysis (MWCO 10 kDa) in the enzyme buffer solutions. The enzyme-polymer labelled conjugate (MEP) was stored at 4°C in the enzyme buffer solution.

A reference enzyme-polymer conjugate (MEP_{ref}) was synthesized following the same procedure described for MEP. Acrylamide (11.69 g, 164 mmol), acryloyl-6-aminocaproic acid (1.94 g, 10.5 mmol), 4,4'-azobis(4-cyanopentanoic acid (28 mg, 0.1 mmol) and 4-cyanopentanoic acid dithiobenzoate (139.7 mg, 0.5 mmol) were dissolved in DMSO (20 mL) and the solution was degassed with N_2 for 30 min. Subsequently the solution was heated at 70°C for 24 h. The reference polymer was purified following the same steps than for MEP. Subsequently, β -gal was covalently attached on the polymer and labelled with FITC following the same procedures described for MEP.

3.3. Synthesis of the multivalent BSA-polymer conjugate (MPP)

The acrylamide-based polymer was synthesized following the same procedure described for MEP. In order to attach the antigen (BSA), the polymer synthesized (1 g L^{-1}) was first dissolved in MES buffer (5 mM, pH 6). Subsequently, the activating agents, 1-ethyl-3-(3-dimethylaminopropyl)carbodiimide (2 mM) and N-hydroxysulfosuccinimide (5 mM) were added to the reaction mixture. The solution was stirred for 15 min at room temperature. In order to purify the activated polymer from reaction by-products, a dialysis (MWCO 3.5 kDa) was performed in MES buffer. Subsequently, BSA (1:1, BSA:polymer, molar ratio) was added to the activated polymer in sodium phosphate buffer (1 M, pH 7.5) for conjugation. The solution was stirred for 2 h at room temperature. The antigen-polymer conjugate was purified by dialysis (MWCO 50 kDa) in a phosphate buffer.

3.4. Synthesis of the *per*-6-iodo- β -cyclodextrin

Triphenylphosphine (40 g, 143 mmol) was dissolved in dry DMF (160 mL). To this solution, iodine (40 g, 160 mmol) was slowly added over 10 min. Subsequently, dry β -CD (11.6 g, 10 mmol) was added to the reaction mixture and the temperature was increased to 70°C. The solution was stirred under N_2 for 20 h. The reaction was cooled to room temperature and was concentrated under reduced pressure. Subsequently sodium methoxide (3 M, 60 mL) was added to the reaction solution while cooling. The solution was stirred for 30 min. The reaction solution was poured in MeOH. The precipitate was washed with MeOH and soxhlet extracted with MeOH for 24 h. The product (15.7 g, 81%) was dried as a white powder.

^1H NMR (CD_3SOCD_3 , 300 MHz): δ = 3.25 (t, 7 H), 3.32-3.45 (m, 14 H), 3.52-3.65 (m, 14 H), 3.78 (d, 7 H), 4.97 (d, 7 H), 5.92 (d, 7 H), 6.03 (d, 7 H); ^{13}C NMR (CD_3SOCD_3 , 75 MHz): δ = 102.0, 86.0, 72.2, 72.0, 71.0, 9.3 ppm

3.5. Synthesis of the *per*-6-azido- β -cyclodextrin

Per-6-iodo- β -cyclodextrin (15 g, 7.9 mmol) was dissolved in DMF (250 mL) and subsequently NaN_3 (5 g, 77.2 mmol) was added to the solution. The mixture was heated to 60°C under N_2 atmosphere and was stirred for 24 h. The reaction mixture was concentrated under reduced pressure and consequently a large excess of water was added. The precipitate powder was filtered, and washed with water. The product (9.2 g, 90%) was dried under vacuum.

^1H NMR (CD_3SOCD_3 , 300 MHz): δ = 3.28-3.40 (m, 14 H), 3.50-3.62 (m, 14 H), 3.65-3.79 (m, 14 H), 4.89 (d, 7 H), 5.75 (d, 7 H), 5.90 (d, 7 H); ^{13}C NMR (CD_3SOCD_3 , 75 MHz): δ = 102.0, 82.8, 73.0, 72.0, 70.5, 51.0 ppm

3.6. Synthesis of the *per*-6-amino- β -cyclodextrin

Per-6-azido- β -cyclodextrin (9 g, 6.8 mmol) was dissolved in DMF (180 mL) and subsequently triphenylphosphine (28.5 g, 108.4 mmol) was added to the solution. The mixture was stirred for 1 h and subsequently concentrated aqueous NH_3 (27 mL, 35%) was added dropwise to the reaction solution. The reaction mixture was stirred for 24 h and subsequently concentrated under reduced pressure. The product was precipitated by addition of EtOH (500 mL). The precipitated powder was washed copiously with EtOH and dried under vacuum (7.1 g, 92%).

^1H NMR (D_2O , 300 MHz): δ = 3.21 (dd, 7 H), 3.39 (dd, 7 H), 3.56 (t, 7 H), 3.64 (dd, 7 H), 3.95 (dd, 7 H), 4.16-4.26 (ddd, 7 H), 5.12 (d, 7 H); ^{13}C NMR (D_2O , 75 MHz): δ = 101.4, 82.1, 72.1, 71.7, 67.8, 40.2 ppm

3.7. Synthesis of 12-(thiodecyl)undecanoic acid

Under anhydrous conditions, sodium (1 g) was added to 100 mL degassed methanol. Dodecanethiol (2 mL, 11.7 mmol) was added to the reaction mixture. Subsequently, 12-bromoundecanoic acid (3.26 g, 11.7 mmol) was added and a clear solution was formed. The reaction mixture was stirred overnight at room temperature under N_2 atmosphere. The product was purified by pouring the reaction mixture in to a solution of water (200 mL), concentrated HCl (10 mL), and diethyl ether (600 mL). The ethereal layer was extracted and washed with deionized water (3 \times 200 mL) and saturated aqueous NaCl (200 mL), dried with anhydrous sodium sulphate, and filtered. Ether was removed under reduced pressure and the compound was purified by crystallization from heptane (2.6 g, yield 56%).

^1H NMR (CDCl_3 , 300 MHz): δ = 2.50 (t, 4 H), 2.35 (t, 2 H), 1.51-1.67 (m, 6 H), 1.18-1.39 (m, 32 H), 0.88 (t, 3 H); ^{13}C NMR (CDCl_3 , 75 MHz): δ = 80.05, 34.06, 32.24, 31.94, 29.76, 29.65, 29.56, 29.52, 29.4, 29.3, 29.27, 29.24, 29.07, 28.97, 24.69, 22.71, 14.12 ppm

3.8. Synthesis of heptakis{6-deoxy-6-[12(thiododecyl)undecanamido]}- β -CD

12-(Thiododecyl)undecanoic acid (1.2 g, 3.1 mmol), *O*-benzotriazol-1-yl-*N,N,N',N'*-tetramethyluronium tetrafluoroborate (TBTU) (1 g, 3.1 mmol) and 4-ethylmorpholine (800 μ l, 6 mmol) were dissolved in dry DMF under anhydrous condition. The reaction mixture was stirred for 10 min at 0°C. The *per*-amino derivative of β -CD (0.5 g, 0.44 mmol) was added to the mixture and the reaction was allowed to warm at room temperature and was stirred for additional 16 h. Consequently, DMF was evaporated under reduced pressure and the residue obtained was dissolved in dichloromethane (200 mL). The reaction solution was extracted with HCl (1 M, 200 mL), water (200 mL) and subsequently dried over magnesium sulphate. Dichloromethane was evaporated under reduced pressure. The residue was re-dissolved in dichloromethane (10 mL) and precipitated in acetone. The product (1 g, yield 60%) was filtered and washed abundantly with acetone.

^1H NMR (CDCl_3 , 300 MHz): δ = 7.26 (s, 7 H), 6.64 (s, 7 H), 5.19 (s, 7 H), 4.87 (s, 7 H), 4.06-3.66 (m, 42 H), 2.49 (t, 28 H), 2.19 (m, 14 H), 1.63-1.48 (m, 42 H), 1.44-1.14 (m, 224 H), 0.88 (t, 21 H); ^{13}C NMR (CDCl_3 , 75 MHz): δ = 174.0, 102.1, 84.2, 73.2, 71.0, 54.1, 43.0, 37.1, 36.1, 32.0, 31.7, 29.7, 29.6, 29.5, 29.3, 29.0, 26.1, 22.5, 14.1 ppm

3.9. Chemical modification of polyethersulfone filtration membranes

Each PES membrane was incubated in an aqueous solution of acrylic acid (2 wt%, 2 mL) for 30 min. Subsequently, the UV photomask was placed on the membrane and UV irradiated (254 nm) under N_2 atmosphere for 2.5 min. The membranes were consequently rinsed with nanopure water. In order to attach covalently the NH-CDs to the surface of the membrane, each AA-PES membrane was incubated in 1 mL solution of NH-CD (0.15 g L^{-1}) and an activating agent (EDC, 10 g L^{-1}) in a phosphate buffer (NaH_2PO_4 50 mM, NaCl 150 mM, pH 7.2) for 2 hours. The reactive sites in excess were blocked using ethanolamine (1 mL, 40 mM). NH-CD-modified membranes (NH-CD-PES) were subsequently stored in nanopure water (resistivity $\geq 18 \text{ M}\Omega \text{ cm}$).

3.10. Chemical modification of gold sensor chip (NH-CD-Au)

In order to clean gold substrates, they were immersed in acetone and subsequently submitted to ultrasonic treatment for 20 min. The same procedure was repeated using

methanol as a solvent. Subsequently, the gold substrates were immersed in a *piranha* solution (H₂SO₄:H₂O₂, 70:30, v/v) for 1 h (WARNING: *piranha* solution is highly oxidative and corrosive; it could explode unexpectedly and must be handled with extreme care). The sensors were then thoroughly rinsed with nanopure water, acetone and were dried under nitrogen. Subsequently the gold substrates were immersed in a solution of heptakis[6-deoxy-6-[12(thiododecyl)undecanamido]]-β-CD (1 mM, EtOH:CHCl₃, 1:2, v/v) overnight. The CD-modified substrates were then rinsed with chloroform and dried under nitrogen.

3.11. Glucose oxidase method

The *O*-dianisidine reagent was prepared by dissolving *O*-dianisidine (25 mg, 0.1 mmol) in 1 mL methanol and adding 49 mL of phosphate buffer (0.1 M, pH 6.5) to this solution. To this mixture, peroxidase (5 mg) and glucose oxidase from *Aspergillus Niger* (5 mg) were added. Subsequently, a freshly prepared *O*-dianisidine reagent was mixed with each sample (1:1, v:v) at 35°C for 40 min. Concentrated hydrochloric acid (6 N, 1:1, v/v) was added to each sample and absorbance was measured at 540 nm.

3.12. Ortho-nitrophenyl-β-galactoside (ONPG) enzymatic assay

50 μl of the enzyme (β-gal) solution was equilibrated for 5 min at 40°C. The substrate solution (ONPG, 50 μl, 40 mM) was added to each sample under stirring for 5 min at 40°C. In order to stop the reaction, the pH was increased using sodium carbonate (1 M, pH 11, 100 μl). Absorbance was measured at 420 nm.

3.13. Microscopic characterization

A Zeiss SUPRA[®] 40VP scanning electron microscope was used for imaging membranes. The PES membranes were dried under ambient conditions, and sputter-coated with a gold-platinum alloy for 30 s at 15 mA using a SC7620 Sputter coater. The SEM micrographs were acquired using the secondary electron mode with an accelerating voltage of 20 kV. Magnification of 10⁴× was used for all the micrographs.

The membrane roughness was measured using a NTEGRA Prima (NT-MDT) atomic force microscopy system and Nova SPM software. The root mean square roughness (RMS) is defined as the standard deviation of the average roughness. The AFM was used in a tapping mode in air and micrographs are presented without any image processing. The AFM system

was equipped with Gold-coated silicon rectangular cantilevers (length 95 μm , width 30 μm , NT-MDT, scan range 25 μm).

3.14. Spectroscopic ellipsometry measurements

Ellipsometry measurements were performed using an imaging and spectroscopic system (EP³ Ellipsometer, Accurion) in a nulling PCSA (polarizer-compensator-sample-analyser) set-up. In this set-up, the incident beam, which is elliptically polarized with a linear polarizer (P) and a quarter-wave plate (C) is reflected from the sample (S) to the analyser (A) and finally imaged with a CCD camera using 10 \times objective. The nulling conditions (related to the optical properties of each sample) were obtained by tuning the angles of P, C and A. Measured data were then converted to the Δ (relative phase shift of *p*- and *s*-polarized light upon reflection on the sample) and ψ (relative amplitude ratio of the reflection coefficients of *p*- and *s*-polarization). Measurements were performed with a fixed angle of incidence (50°) at five different wavelengths ($\lambda=629.3, 760.3, 829.9, 905.0, 1000.8$ nm). Thickness of transferred layers was calculated by transferring measured Δ and ψ as a function of wavelength λ to the EP⁴ model software. A model with two layers (AU/CD-SAM/air) was created. Using data base of EP⁴ software, dispersion functions of Au and air as ambient were defined. A Cauchy model with predefined refractive index and extinction coefficient ($n= 1.5, k=0$) was designated for the CD-SAM. Thickness of 22 Å was measured for CD-SAM layer. A system control was done prior to each set of experiments using standard Au samples.

Chapter 4. Conclusion

In the frame of this PhD research work we developed a new supramolecular strategy that allows immobilizing enzymes at the surface of filtration membranes in a stable and reversible fashion. Our approach is based on multiple points host-guest supramolecular inclusion interactions between CDs immobilized at the surface of the PES membranes and enzyme-polymer conjugates. Low density of CDs host entities were immobilized covalently at the surface of the polymeric filtration membrane following a coupling reaction between activated carboxylic acids on PES surfaces and primary amine functions of the *per*-amino derivative of β -CD (NH-CD). No significant differences in morphology, roughness and water flow through the membrane was observed, which confirmed that the physico-chemical properties of filtration membranes did not change drastically after immobilization of CDs.

As a multivalent enzyme-polymer conjugate, we synthesized an acrylamide-based polymer possessing adamantyl moieties as guest functions and β -gal as a biocatalyst. The membrane bioreactors developed in this research work, with immobilized β -gal at the surface of PES membranes, allowed for an efficient hydrolysis of lactose in milk serum. For future applications, in order to increase the bio-catalytic conversion rate at the surface of the filtration membrane, the immobilized enzyme density should be increased at the surface. This can be achieved using star-, comb- or brush-based polymer instead of the used linear polymer and therefore increasing the number of the chemical moieties for covalent anchoring of the enzyme.

The used bio-conjugation strategy is versatile as it is based on a coupling reaction between activated carboxylic acids of the polymer and primary amine functions of lysine residues of the enzyme and can therefore be applied to a wide range of enzymes. Some commercially available enzymes, which are used in industrial-scale production bioprocesses, are amylases, lipases, proteases, laccase, cellulases, *etc.*. For instance, amylases can be used for the conversion of starch to sugar syrups, and production of CDs for pharmaceutical or food industries. Other widely used industrial bio-catalysts are Lipases. They can be used in

detergents and waste water treatments for degradation of fat containing materials. Cellulases have the ability to degraded lignocellulosic feedstocks and therefore are widely used in textile industries. Another industrial applicable enzyme is laccases, which is used for bleaching in paper and textile industries. Our developed strategy can be applied to immobilize different enzymes that are used in variety of industrial sectors such as textile, dairy, baking, pulp and paper, beverage, brewing and cosmetic industries, to name but a few.

We applied a similar supramolecular approach used for reversible modification of filtration membranes for reversible bio-functionalization of gold surfaces, which were used to prepare sensor chips for surface plasmon resonance assays. A self-assembled monolayer of the dialkylsulfide derivative of β -CD was prepared on a surface of Au sensor chips.

In order to produce a multivalent protein-polymer conjugate guest molecule, we synthesized an acrylamide-based polymer (MPP), possessing adamantyl moieties as guest functions and BSA as a ligand. This was achieved following the same synthetic route used for MEP. This approach allowed for the stable but yet reversible immobilization of BSA at the surface of an Au SPR sensor chip. The MPP-modified SPR sensor chip allowed the assessment of an efficient antigen-antibody interaction. We demonstrated that the surface of the BSA-modified sensors could be regenerated after injection of β -CD as a competitor host. We repeated the MPP binding assay and confirmed the possibility to modify and regenerate the surface of Au SPR sensor chips with MPP without significant loss of antigen-antibody affinity.

The efficiency of antigen-antibody recognition based on this strategy may be improved by increasing the density of immobilized protein at the surface of the sensor chip. This can be achieved, following a similar approach that was mentioned above for increasing the bio-catalytic conversion rate at the surface of the membranes, using star-, comb- or brush-based polymer and therefore increasing the number of the immobilized proteins. This strategy can also be extended to immobilize antibodies instead of antigens on the surface of SPR sensors. Indeed, antibodies are one of the most widely used biological recognition molecules in SPR biosensors. In the case of an antibody-antigen interaction, immobilization of antibodies at the surface of SPR sensor chips would avoid the binding avidity effects that result from the bivalency of the antibody. Immobilization of the bivalent protein allows determination of the kinetic rate constants by fitting the responses to a simple Langmuir

binding model. This approach can be theoretically used to immobilize a large variety of ligands on surface of SPR sensor chips and will allow using the same SPR sensor chip for several different immunoassays. This method can also be adapted to covalently immobilize CD derivatives at the surface of other SPR sensor chips such as carboxymethylated dextran-modified (CM) sensors. The CM sensors can be chemically modified using a coupling reaction between activated carboxylic acids of the sensor's surface and primary amine functions of an amino derivative of β -CD.

Our developed method theoretically allows the stable but yet reversible immobilization of any type of enzyme at the surface of different carrier materials (*e.g.* nanoparticles). This approach is expected to be important for different industrial bio-based applications.

References

1. C. Fasting, C. A. Schalley, M. Weber, O. Seitz, S. Hecht, B. Kokschi, J. Dervedde, C. Graf, E.-W. Knapp and R. Haag, *Angew. Chem., Int. Ed.*, 2012, **51**, 10472-10498.
2. A. Mulder, J. Huskens and D. N. Reinhoudt, *Org. Biomol. Chem.*, 2004, **2**, 3409-3424.
3. M. V. Rekharsky and Y. Inoue, *Chem. Rev.*, 1998, **98**, 1875-1917.
4. J. L. Atwood and J. M. Lehn, *Comprehensive Supramolecular Chemistry: Cyclodextrins*, Pergamon, 1996.
5. A. R. Khan, P. Forgo, K. J. Stine and V. T. D'Souza, *Chem. Rev.*, 1998, **98**, 1977-1996.
6. C. J. Easton and S. F. Lincoln, *Modified Cyclodextrins: Scaffolds and Templates for Supramolecular Chemistry*, Imperial College Press, 1999.
7. D. Q. Yuan, T. Tahara, W. H. Chen, Y. Okabe, C. Yang, Y. Yagi, Y. Nogami, M. Fukudome and K. Fujita, *J. Org. Chem.*, 2003, **68**, 9456-9466.
8. T. Auletta, B. Dordi, A. Mulder, A. Sartori, S. Onclin, C. M. Bruinink, M. Peter, C. A. Nijhuis, H. Beijleveld, H. Schonherr, G. J. Vancso, A. Casnati, R. Ungaro, B. J. Ravoo, J. Huskens and D. N. Reinhoudt, *Angew. Chem., Int. Ed.*, 2004, **43**, 369-373.
9. M. J. W. Ludden, D. N. Reinhoudt and J. Huskens, *Chem. Soc. Rev.*, 2006, **35**, 1122-1134.
10. P. Maury, M. Peter, O. Crespo-Biel, X. Y. Ling, D. N. Reinhoudt and J. Huskens, *Nanotechnology*, 2007, **18**, 44007.
11. C. A. Nijhuis, J. K. Sinha, G. Wittstock, J. Huskens, B. J. Ravoo and D. N. Reinhoudt, *Langmuir*, 2006, **22**, 9770-9775.
12. A. Villiers, *Compt. Rend. Fr. Acad. Sci*, 1891, **112**, 435-438.
13. R. P. Walton, *A comprehensive survey of starch chemistry*, Chemical Catalog Company, New York, 1928.
14. H. Pringsheim, *The Chemistry of the Monosaccharides and of the Polysaccharides*, McGraw-Hill Book Company, New York, 1932.
15. H. Pringsheim, *The dextrans: Characteristics, sources, and properties.*, McGraw-Hill Book Company, New York, 1932.
16. K. Freudenberg, G. Blomquist, L. Ewald and K. Soff, *Ber. Dtsch. Chem. Ges.*, 1936, **69**.
17. F. Cramer, *Einschlussverbindungen*, Springer, 1954.
18. K. Lindner and W. Saenger, *Carbohydr. Res.*, 1982, **99**, 103-115.
19. F. Shiraishi, K. Kawakami, H. Marushima and K. Kusunoki, *Starch/Staerke*, 1989, **41**, 151-155.
20. K. A. Connors, *Chem. Rev.*, 1997, **97**, 1325-1357.
21. P. Shahgaldian and U. Pieleles, *Sensors*, 2006, **6**, 593-615.
22. Y. Xiao, S. C. Ng, T. T. Y. Tan and Y. Wang, *J. Chromatogr., A*, 2012, **1269**, 52-68.
23. J. Mosinger, V. Tomankova, I. Nemcova and J. Zyka, *Anal. Lett.*, 2001, **34**, 1979-2004.
24. E. Schneiderman and A. M. Stalcup, *J. Chromatogr., B*, 2000, **745**, 83-102.
25. H. Nishi, *J. Chromatogr., A*, 1997, **792**, 327-347.
26. F. Bressolle, M. Audran, T. N. Pham and J. J. Vallon, *J. Chromatogr., B*, 1996, **687**, 303-336.

27. J. Szejtli, *Chem. Rev.*, 1998, **98**, 1743-1754.
28. A. Biber, G. Antranikian and E. Heinzle, *Appl. Microbiol. Biotechnol.*, 2002, **59**, 609-617.
29. S. Kobayashi, *Biotechnol. Prog.*, 1996, **12**, 23-41.
30. H. Bender, *Adv. Biotechnol. Process.*, 1986, **6**, 37-71.
31. P. Mattsson, T. Korpela, S. Paavilainen and M. Mäkelä, *Appl. Biochem. Biotechnol.*, 1991, **30**, 17-28.
32. J.-H. Lee, K.-H. Choi, J.-Y. Choi, Y.-S. Lee, I.-B. Kwon and J.-H. Yu, *Enzyme Microb. Technol.*, 1992, **14**, 1017-1020.
33. G. Schmid, in *Comprehensive supermolecular chemistry*, Pergamon, Oxford, 1996, pp. 41-56.
34. J. Szejtli, *Chem. Rev.*, 1998, **98**, 1743-1754.
35. A. Hedges, in *Starch Hydrolysis Products*, eds. Fred W. Schenck and R. E. Hebeda, VCH Publishers, New York, 1992, pp. 319-333.
36. H.-J. Schneider, F. Hackett, V. Ruediger and H. Ikeda, *Chem. Rev.*, 1998, **98**, 1755-1786.
37. J. García, L. Martins and M. Pons, *NMR Spectroscopy in Solution*, John Wiley & sons, Chichester, 2013.
38. K. Harata, *Crystallographic studies*, Pergamon Press, Oxford, 1996.
39. R. Singh, N. Bharti, J. Madan and S. N. Hiremath, *J. Pharm. Sci. Technol.*, 2010, **2**, 171-183.
40. G. Ercolani, *J. Am. Chem. Soc.*, 2003, **125**, 16097-16103.
41. M. L. Wolfenden and M. J. Cloninger, *J. Am. Chem. Soc.*, 2005, **127**, 12168-12169.
42. D. Philp and J. F. Stoddart, *Angew. Chem. Int. Ed.*, 1996, **35**, 1155-1196.
43. A. P. Bisson, F. J. Carver, C. A. Hunter and J. P. Waltho, *J. Am. Chem. Soc.*, 1994, **116**, 10292-10293.
44. M. Mammen, S. K. Choi and G. M. Whitesides, *Angew. Chem. Int. Ed.*, 1998, **37**, 2755-2794.
45. P. I. Kitov and D. R. Bundle, *J. Am. Chem. Soc.*, 2003, **125**, 16271-16284.
46. H. Jacobson and W. H. Stockmayer, *J. Chem. Phys.*, 1950, **18**, 1600-1606.
47. M. J. Cloninger, B. Bilgiçer, L. Li, S. L. Mangold, S. T. Phillips and M. L. Wolfenden, *Multivalency*, John Wiley & Sons, Chichester, 2012.
48. I. Beletskaya, V. S. Tyurin, A. Y. Tsivadze, R. Guillard and C. Stern, *Chem. Rev.*, 2009, **109**, 1659-1713.
49. H. L. Anderson, S. Anderson and J. K. M. Sanders, *J. Chem. Soc., Perkin Trans. 1*, 1995, 2231-2245.
50. V. Balzani, M. Clemente-León, A. Credi, J. N. Lowe, J. D. Badjić, J. F. Stoddart and D. J. Williams, *Chem.--Eur. J.*, 2003, **9**, 5348-5360.
51. J. Rao, J. Lahiri, L. Isaacs, R. M. Weis and G. M. Whitesides, *Science*, 1998, **280**, 708-711.
52. J. Rao, J. Lahiri, R. M. Weis and G. M. Whitesides, *J. Am. Chem. Soc.*, 2000, **122**, 2698-2710.
53. A. Mulder, T. Auletta, A. Sartori, S. Del Ciotto, A. Casnati, R. Ungaro, J. Huskens and D. N. Reinhoudt, *J. Am. Chem. Soc.*, 2004, **126**, 6627-6636.
54. C. T. Sikorski and R. C. Petter, *Tetrahedron Lett.*, 1994, **35**, 4275-4278.
55. Y. Liu, Y. Chen, B. Li, T. Wada and Y. Inoue, *Chem.--Eur. J.*, 2001, **7**, 2528-2535.

56. Y. Liu, Li, H.-Y. Zhang and Y. Song, *J. Org. Chem.*, 2003, **68**, 527-536.
57. Y. Liu, B. Li, C.-C. You, T. Wada and Y. Inoue, *J. Org. Chem.*, 2001, **66**, 225-232.
58. R. Breslow, S. Halfon and B. Zhang, *Tetrahedron*, 1995, **51**, 377-388.
59. R. Breslow and S. Chung, *J. Am. Chem. Soc.*, 1990, **112**, 9659-9660.
60. A. Mulder, A. Juković, F. W. B. van Leeuwen, H. Kooijman, A. L. Spek, J. Huskens and D. N. Reinhoudt, *Chem.--Eur. J.*, 2004, **10**, 1114-1123.
61. A. Mulder, A. Jukovic, J. Huskens and D. N. Reinhoudt, *Org. Biomol. Chem.*, 2004, **2**, 1748-1755.
62. A. Mulder, A. Jukovic, L. N. Lucas, J. van Esch, B. L. Feringa, J. Huskens and D. N. Reinhoudt, *Chem. Commun.*, 2002, 2734-2735.
63. J. C. Love, L. A. Estroff, J. K. Kriebel, R. G. Nuzzo and G. M. Whitesides, *Chem. Rev.*, 2005, **105**, 1103-1169.
64. M. T. Rojas, R. Koniger, J. F. Stoddart and A. E. Kaifer, *J. Am. Chem. Soc.*, 1995, **117**, 336-343.
65. G. Nelles, M. Weisser, R. Back, P. Wohlfart, G. Wenz and S. Mittler-Neher, *J. Am. Chem. Soc.*, 1996, **118**, 5039-5046.
66. M. W. J. Beulen, J. Bugler, B. Lammerink, F. A. J. Geurts, E. M. E. F. Biemond, K. G. C. van Leerdam, F. C. J. M. van Veggel, J. F. J. Engbersen and D. N. Reinhoudt, *Langmuir*, 1998, **14**, 6424-6429.
67. P. Shahgaldian, M. Hegner and U. Pielers, *J. Incl. Phenom. Macro.*, 2005, **53**, 35-39.
68. S. Onclin, A. Mulder, J. Huskens, B. J. Ravoo and D. N. Reinhoudt, *Langmuir*, 2004, **20**, 5460-5466.
69. T. Auletta, B. Dordi, A. Mulder, A. Sartori, S. Onclin, C. M. Bruinink, M. Peter, C. A. Nijhuis, H. Beijleveld, H. Schönherr, G. J. Vancso, A. Casnati, R. Ungaro, B. J. Ravoo, J. Huskens and D. N. Reinhoudt, *Angew. Chem., Int. Ed.*, 2004, **43**, 369-373.
70. J. Huskens, M. A. Deij and D. N. Reinhoudt, *Angew. Chem., Int. Ed.*, 2002, **41**, 4467.
71. M. J. W. Ludden, D. N. Reinhoudt and J. Huskens, *Chem. Soc. Rev.*, 2006, **35**, 1122-1134.
72. M. J. W. Ludden, X. Li, J. Greve, A. van Amerongen, M. Escalante, V. Subramaniam, D. N. Reinhoudt and J. Huskens, *J. Am. Chem. Soc.*, 2008, **130**, 6964-6973.
73. M. L. W. Ludden, A. Mulder, K. Schulze, V. Subramaniam, R. Tampe and J. Huskens, *Chem. Eur. J.*, 2008, **14**, 2044-2051.
74. S. Onclin, J. Huskens, B. J. Ravoo and D. N. Reinhoudt, *Small*, 2005, **1**, 852-857.
75. C. M. Bruinink, C. A. Nijhuis, M. Péter, B. Dordi, O. Crespo-Biel, T. Auletta, A. Mulder, H. Schönherr, G. J. Vancso, J. Huskens and D. N. Reinhoudt, *Chem.--Eur. J.*, 2005, **11**, 3988-3996.
76. L. T. Yang, A. Gomez-Casado, J. F. Young, H. D. Nguyen, J. Cabanas-Danes, J. Huskens, L. Brunsveld and P. Jonkheijm, *J. Am. Chem. Soc.*, 2012, **134**, 19199-19206.
77. A. González-Campo, B. Eker, H. J. G. E. Gardeniers, J. Huskens and P. Jonkheijm, *Small*, 2012, **8**, 3531-3537.
78. A. Gonzalez-Campo, S. H. Hsu, L. Puig, J. Huskens, D. N. Reinhoudt and A. H. Velders, *J. Am. Chem. Soc.*, 2010, **132**, 11434-11436.
79. A. Harada, R. Kobayashi, Y. Takashima, A. Hashidzume and H. Yamaguchi, *Nat. Chem.*, 2011, **3**, 34-37.
80. K. Drauz, H. Gröger and O. May, *Enzyme catalysis in organic synthesis: a comprehensive handbook*, Wiley-VCH, Weinheim, 2012.

81. W. Aehle, *Enzymes in industry; production and applications*, Wiley-VCH, Weinheim, 2007.
82. M. B. Quin and C. Schmidt-Dannert, *ACS Catal.*, 2011, **1**, 1017-1021.
83. A. Schmid, J. S. Dordick, B. Hauer, A. Kiener, M. Wubbolts and B. Witholt, *Nature*, 2001, **409**, 258-268.
84. E. Drioli and L. Giorno, *Membrane reactors: applications in biotechnology and the pharmaceutical industry*, Taylor & Francis, London, 1999.
85. J. Agustian, A. H. Kamaruddin and S. Bhatia, *Chem. Technol. Biotechnol.*, 2011, **86**, 1032-1048.
86. P. Jochems, Y. Satyawali, L. Diels and W. Dejonghe, *Green Chem.*, 2011, **13**, 1609-1623.
87. J. F. Ma, L. H. Zhang, Z. Liang, W. B. Zhang and Y. K. Zhang, *Anal. Chim. Acta*, 2009, **632**, 1-8.
88. N. Moridi, P. F. X. Corvini and P. Shahgaldian, *Angew. Chem. Int. Ed.*, 2015, **(in press)**.
89. K. Mohanty and M. K. Purkait, *Membrane Technologies and Applications*, CRC Press, Boca Raton, 2011.
90. C. van Rijn, *Nano and Micro Engineered Membrane Technology*, Elsevier Science, Amsterdam, 2004.
91. D. S. Wavhal and E. R. Fisher, *Langmuir*, 2002, **19**, 79-85.
92. S. P. Nunes and K. V. Peinemann, *Membrane Technology: in the Chemical Industry*, Wiley-VCH, Weinheim, 2006.
93. J. Schauer, W. Albrecht, T. Weigel, V. Kudela and Z. Pientka, *J. Appl. Polym. Sci.*, 2001, **81**, 134-142.
94. M. Duke, D. Zhao, R. Semiat and M. Lu, *Functional Nanostructured Materials and Membranes for Water Treatment*, Wiley-VCH, Weinheim, 2013.
95. H. Susanto and M. Ulbricht, *Langmuir*, 2007, **23**, 7818-7830.
96. H. R. Luckarift, J. C. Spain, R. R. Naik and M. O. Stone, *Nat. Biotechnol.*, 2004, **22**, 211-213.
97. D. Brady and J. Jordaan, *Biotechnol. Lett.*, 2009, **31**, 1639-1650.
98. N. Hilal, V. Kochkodan, R. Nigmatullin, V. Goncharuk and L. Al-Khatib, *J. Membr. Sci.*, 2006, **268**, 198-207.
99. L. Giorno, R. Molinari, M. Natoli and E. Drioli, *J. Membr. Sci.*, 1997, **125**, 177-187.
100. J. L. Lopez and S. L. Matson, *J. Membr. Sci.*, 1997, **125**, 189-211.
101. M. N. Abu Seman, M. Khayet, Z. I. Bin Ali and N. Hilal, *J. Membr. Sci.*, 2010, **355**, 133-141.
102. P. R. Ashton, R. Königer, J. F. Stoddart, D. Alker and V. D. Harding, *J. Org. Chem.*, 1996, **61**, 903-908.
103. G. Moad and C. Barner-Kowollik, *Handbook of RAFT polymerization*, Wiley-VCH, Weinheim, 2008.
104. M. Rubio-Teixeira, *Biotechnol. Adv.*, 2006, **24**, 212-225.
105. E. Wijaya, C. Lenaerts, S. Maricot, J. Hastanin, S. Habraken, J.-P. Vilcot, R. Boukherroub and S. Szunerits, *Curr. Opin. Solid State Mater. Sci.*, 2011, **15**, 208-224.
106. R. B. M. Schasfoort and A. J. Tudos, *Handbook of Surface Plasmon Resonance*, Royal Society of Chemistry, Cambridge, 2008.
107. R. Wang, A. Lajevardi-Khosh, S. Choi and J. Chae, *Biosens. Bioelectron.*, 2011, **28**, 304-307.
108. G. A. Campbell and R. Mutharasan, *Biosens. Bioelectron.*, 2006, **22**, 78-85.
109. A. W. Drake and S. L. Klakamp, *J. Immunol. Methods*, 2011, **371**, 165-169.

110. E. B. Troughton, C. D. Bain, G. M. Whitesides, R. G. Nuzzo, D. L. Allara and M. D. Porter, *Langmuir*, 1988, **4**, 365-385.
111. P. Shahgaldian, M. Hegner and U. Pieleles, *J. Inclusion Phenom. Macrocyclic Chem.*, 2005, **53**, 35-39.

MORIDI Negar

Im Eigen 3
5080 Laufenburg
32, female

☎ : +41-79-534 66 34

✉ : negar.moridi@bluewin.ch



EDUCATION

- 2011-present** • **PhD student in Nano and Micro Technology:** Ecole Polytechnique Fédérale de Lausanne and University of Applied Sciences Northwestern Switzerland
- 2009-2011** • **Master of Science in Life Sciences:** University of Applied Sciences Northwestern Switzerland
- 2007-2009** • **Master of Advanced studies in Nano- and Micro Technology:** University of Applied Sciences and Arts Western Switzerland with honors
- 2006-2007** • **Certificat d'études francaises:** University of Neuchâtel, Switzerland
- 2002-2006** • **B.Sc. in industrial Chemical Engineering:** University of Guilan, (Iran)

PROFESSIONAL EXPERIENCE

- 2011-present** • **PhD thesis:** Reversible supramolecular modification of surfaces. (*Muttenz FHNW and Lausanne EPFL*)
- 2010-2011** • **Master thesis:** Polymorphism control of active pharmaceutical ingredients using nano-structured surfaces. (*Muttenz FHNW, 8 months*)
- 2009-2011** • **Research Assistant, Dept. Of Chemistry and Bio-analytics, University of Applied Sciences Northwestern Switzerland (FHNW):** I work as part of Prof. Dr. Patrick Shahgaldian research group in the field of nanotechnology. The research project was about the study of self-assembled properties of series of complexes amphiphiles and their ability to template crystal growths.
- 2008-2009** • **Master of Advanced thesis:** Supramolecular nano-particulate systems for molecular recognition. (*Muttenz FHNW, 4 months*)
- 2005-2006** • **Bachelor thesis:** Improvement of drying quality in food industry by using D.O.E technique. In cooperation of University of Tehran and Guilan. (*Iran, 4 months*)
- 2004-2005** • **Internship, BR. SA:** Worked as chemical student in chemical laboratory of Bandar-Abbas refinery. I had different tasks in refinery and quality control room laboratory. (*Iran, 3 months*)

TECHNICAL SKILLS

- **Analytical techniques:** NMR, MALDI-MS, Raman & IR spectroscopy
- **Surface analysis methods:** AFM, SEM, Spectroscopic ellipsometry
- **Coating technique:** Langmuir-Blodgett

PUBLICATIONS, PATENT AND AWARD

- Moridi N., Corvini P. F. X., Shahgaldian P., Reversible Supramolecular Surface Attachment of Enzyme-Polymer Conjugates for the Design of Biocatalytic Filtration Membranes. *Angew. Chem. Int. Ed.* **2015**, DOI: 10.1002/anie.201507020.
- Shahgaldian, P., Corvini, P. F.-X., Dudal, Y, Moridi N., Method of reversibly functionalizing a solid surface. European Patent, **2015**, EP15166312.7.
- Correro R., Moridi N., Schützinger H., Sykora S., Corvini P. F. X., Shahgaldian P., Enzyme Shielding in an Enzyme-thin and Soft Organosilica Layer **2015**, (*submitted*).
- El Idrissi, M.; Moridi, N.; Shahgaldian, P., Function-Oriented Molecular Design of Cyclodextrins In *Encyclopedia of Physical Organic Chemistry*, W. Zherong, Ed. Wiley-VCH, Weinheim: 2015, (*in press*).
- Rullaud, V., Moridi, N. & Shahgaldian, P. Sequence-Specific DNA Interactions with Calixarene-Based Langmuir Monolayers. *Langmuir* **2014**, 30, 8675-8679.
- Tulli, L. G., Moridi, N., Wang, W., Helttunen, K., Neuburger, M., Vaknin, D., Meier, W., Shahgaldian, P., Polymorphism control of an active pharmaceutical ingredient beneath calixarene-based Langmuir monolayers. *Chem. Commun.* **2014**, 50, 3938-3940.
- Student and post-doc travel awards, 8th International symposium on macrocyclic and supramolecular Chemistry **2013**.
- Moridi, N., Wackerlin, C., Rullaud, V., Schelldorfer, R., Jung, T. A., Shahgaldian, P., Langmuir-Blodgett monolayer stabilization using supramolecular clips. *Chem. Commun.* **2013**, 49, 367-369.
- Helttunen, K., Moridi, N., Shahgaldian, P., Nissinen, M., Resorcinarene bis-crown silver complexes and their application as antibacterial Langmuir-Blodgett films. *Org. Biomol. Chem.* **2012**, 10, 2019-2025.
- Moridi, N., Danylyuk, O., Suwinska, K., Shahgaldian, P., Monolayers of an amphiphilic *para*-carboxy-calix[4]arene act as templates for the crystallization of acetaminophen. *J. Colloid Interface Sci.* **2012**, 377, 450-455.
- Moridi, N., Elend, D., Danylyuk, O., Suwinska, K., Shahgaldian, P., Amidophenol-Modified Amphiphilic Calixarenes: Synthesis, Interfacial Self-Assembly, and Acetaminophen Crystal Nucleation Properties. *Langmuir* **2011**, 27, 9116-9121.

LANGUAGES

French:	good spoken and written
English:	good spoken and written
German:	Basic knowledge
Persian:	native language

HOBBIES

- Dancing, biking, swimming, fitness